Downloaded from http://jgs.lyellcollection.org/ at Universitats- und Landesbibliothek Munster on September 16, 2020

Accepted Manuscript

*Journal of the Geological Society*

# Uncharted Permian to Jurassic continental deposits in the far north of Victoria Land, East Antarctica

Benjamin Bomfleur, Thomas Mörs, Jan Unverfärth, Feng Liu, Andreas Läufer, Paula Castillo, Changhwan Oh, Tae-Yoon S. Park, Jusun Woo & Laura Crispini

DOI: https://doi.org/10.1144/jgs2020-062

To access the most recent version of this article, please click the DOI URL in the line above.

Received 2 April 2020
Revised 20 August 2020
Accepted 8 September 2020

© 2020 The Author(s). Published by The Geological Society of London. All rights reserved. For permissions: http://www.geolsoc.org.uk/permissions. Publishing disclaimer: www.geolsoc.org.uk/pub_ethics

Supplementary material at https://doi.org/10.6084/m9.figshare.c.5118431

When citing this article please include the DOI provided above.

**Manuscript version: Accepted Manuscript**
This is a PDF of an unedited manuscript that has been accepted for publication. The manuscript will undergo copyediting, typesetting and correction before it is published in its final form. Please note that during the production process errors may be discovered which could affect the content, and all legal disclaimers that apply to the journal pertain.

Although reasonable efforts have been made to obtain all necessary permissions from third parties to include their copyrighted content within this article, their full citation and copyright line may not be present in this Accepted Manuscript version. Before using any content from this article, please refer to the Version of Record once published for full citation and copyright details, as permissions may be required.

Downloaded from http://jgs.lyellcollection.org/ at Universitats- und Landesbibliothek Munster on September 16, 2020

# Uncharted Permian to Jurassic continental deposits in the far north of Victoria Land, East Antarctica

Benjamin Bomfleur[1]*, Thomas Mörs[2], Jan Unverfärth[1], Feng Liu[3], Andreas Läufer[4], Paula Castillo[1], Changhwan Oh[5], Tae-Yoon S. Park[6], Jusun Woo[7], and Laura Crispini[8]

[1]Institute for Geology and Palaeontology, Westfälische Wilhelms-Universität Münster, 48147 Münster, Germany

[2]Department of Palaeobiology, Swedish Museum of Natural History, 10405 Stockholm, Sweden

[3]State Key Laboratory of Palaeobiology and Stratigraphy, Nanjing Institute of Geology and Palaeontology and Center for Excellence in Life and Paleoenvironment, Nanjing 210008, China

[4]Federal Institute for Geosciences and Natural Resources (BGR), 30655 Hannover, Germany

[5]Department of Earth Sciences Education, Chungbuk National University, Chungbuk 28644, Republic of Korea

[6]Division of Polar Earth-System Sciences, Korea Polar Research Institute, Incheon 21990, Republic of Korea

[7]School of Earth and Environmental Sciences, Seoul National University, Seoul 21990, Republic of Korea

[8]DISTAV, University of Genova, 16132 Genova, Italy

*Correspondence (bbomfleur@uni-muenster.de)

Running title: Beacon Supergroup in northern Victoria Land

ACCEPTED MANUSCRIPT

Downloaded from http://jgs.lyellcollection.org/ at Universitats- und Landesbibliothek Munster on September 16, 2020

***Abstract***

The remote lower reaches of the Rennick Glacier in the far north of Victoria Land hold some of the least explored outcrop areas of the Transantarctic basin system. Following recent international field-work efforts in the Helliwell Hills, we here provide a comprehensive emendation to the regional stratigraphy. Results of geological and palaeontological reconnaissance and of petrographic, geochemical, and palynostratigraphic analyses reveal a stack of three previously unknown sedimentary units in the study area: the Lower Triassic Van der Hoeven Formation (new unit, 115+ m thick) consists mainly of quartzose sandstone and non-carbonaceous mudstone rich in continental trace fossils. The Middle to Upper Triassic Helliwell Formation (new unit, 235 m thick) consists of coal-bearing overbank deposits and volcaniclastic sandstone and yielded typical plant fossils of the Gondwanan *Dicroidium* flora together with plant-bearing silicified peat. The succession is capped by *c*. 14 m of the sandstone-dominated Section Peak Formation (?uppermost Triassic–Lower Jurassic). Our results enable more detailed correlation of the Palaeozoic–Mesozoic successions throughout East Antarctica and into Tasmania. Of particular interest is one section that spans the end-Permian mass extinction interval, which promises to allow detailed reconstructions of high-latitude vegetation dynamics across this critical interval in Earth History.

[*end of abstract*]

A Supplementary Data File containing supplementary information, figures S1–S7, and additional references is available at https://doi.org/10.6084/m9.figshare.c.5118431

ACCEPTED MANUSCRIPT

Downloaded from http://jgs.lyellcollection.org/ at Universitats- und Landesbibliothek Munster on September 16, 2020

The Beacon Supergroup ("Beacon Sandstone" of Ferrar 1907) forms the infill of the Transantarctic basin (Elliot 1975), a continental sedimentary basin system that extended over 3000 km along the active Panthalassan margin of high-latitude Gondwana from the late Palaeozoic until at least the Jurassic (Elliot 1975; Barrett 1991; Collinson *et al.* 1994; Goodge 2020). Today, sedimentary deposits of the Beacon Supergroup are exposed along the entire Transantarctic Mountains, from Victoria Land in the east across the central Transantarctic Mountains into isolated outcrop areas along the western perimeter of the East Antarctic cratonic assemblage (Barrett 1991; Collinson *et al.* 1994; Goodge 2020).

One of the least-explored regions of the Transantarctic basin system lies in the far north of Victoria Land in the lower Rennick Glacier area, a remote and rarely visited terrain of isolated mountain ranges that flank Earth's second-largest outlet glacier. After the earliest en-route reconnaissance in the "Heroic Age of Antarctic Exploration" (see Borchgrevink 1901; Rastall and Priestley 1921), the first mainland visits along the Oates and Pennell coasts were conducted only about fifty years later during ship-based surveys by Russian (Klimov and Soloviev 1958; Soloviev 1960) and Australian scientists (McLeod 1964). New Zealand and United States Geological Survey expeditions later launched sledging surveys and helicopter reconnaissance farther inland (e.g., Harrington *et al.* 1964, 1967; LeCouteur and Leitch 1964; Crowder 1968), which eventually resulted in the first geological maps depicting also the Beacon Supergroup deposits of the lower Rennick Glacier region (Crowder 1968; Gair *et al.* 1969; Sturm and Carryer 1970) (Fig. 1). More detailed stratigraphic descriptions appeared following extensive international field-work efforts during the late 1960s to early 1980s (Dow and Neall 1972, 1974; Skinner 1981; Walker 1983; Collinson and Kemp 1983; Collinson *et al.* 1986). Only a few contributions to the regional stratigraphy have been made since then (John 2014; Schöner and John 2014; Cornamusini *et al.* 2017).

The Beacon Supergroup deposits in the lower Rennick Glacier area (Fig. 1) have thus far been known to consist almost exclusively of siliciclastic fluvio-lacustrine deposits assigned to the Takrouna Formation (Dow and Neall 1974; Collinson *et al.* 1986; John 2014; Schöner and John 2014). Local occurrences of glacigenic deposits underlying the Takrouna Formation in the Orr Glacier area, Lanterman Range (Laird and Bradshaw 1981; Skinner 1981; McKelvey and Walker 1983), have only recently been

ACCEPTED MANUSCRIPT

Downloaded from http://jgs.lyellcollection.org/ at Universitats- und Landesbibliothek Munster on September 16, 2020

described as a separate stratigraphic unit, namely the Lanterman Formation (Cornamusini *et al.* 2017). The precise age ranges of both formations remain poorly constrained. A preliminary age assessment of a microflora from the northern Alamein Range (Norris pers. comm. *in* Sturm and Carryer 1970, p. 432; see Fig. 1) has been taken to indicate a probable Late Triassic age for part of the Takrouna Formation. Multiple reports of *Vertebraria* roots, glossopterid leaves, and an associated *Plumsteadia*-like reproductive organ—all typical for the Permian of Gondwana—have since consistently indicated a Permian age for the formation (Dow and Neall 1972, 1974; Hammer and Zawiskie 1982; Collinson and Kemp 1983; Walker 1983; Collinson *et al.* 1986; Hammer 1986; Tessensohn and Mädler 1987). Recently, a poorly preserved palynomorph assemblage from a sample of primary-matrix (i.e., non-reworked) mudstone within the Lanterman Formation revealed an earliest Permian (Asselian) age for the glacigenic deposits beneath the Takrouna Formation (Cornamusini *et al.* 2017). Compared to the well-exposed and well-studied sections of the Devonian to Jurassic Beacon Supergroup in the central Transantarctic Mountains and in southern Victoria Land (see, e.g., Barrett 1991; Collinson *et al.* 1994; Elliott *et al.* 2017), the preserved sedimentary record of the Transantarctic basin system in the study area has thus appeared to be fragmentary.

As a result of joint international field-work efforts during austral summers 2014-2015 and 2015-2016, previously uncharted sedimentary deposits were discovered in the Helliwell Hills in the lower Rennick Glacier region. Characteristic lithological features and fossil content of these deposits enable us to distinguish four continental sedimentary units, including two new formations of Early Triassic and of mid- to Late Triassic age, respectively. Our revision of the regional stratigraphy provides crucial tie-points for basin-wide correlation and reveals a potentially continuous section across the Permian-Triassic boundary as a prime future target to study biotic and environmental changes through the end-Permian biotic crisis in terrestrial high-latitude palaeoecosystems.

ACCEPTED MANUSCRIPT

Downloaded from http://jgs.lyellcollection.org/ at Universitats- und Landesbibliothek Munster on September 16, 2020

## Materials and Methods

### *Locality descriptions*

*Boggs Valley*.—Boggs Valley is a large, trough-shaped, southwest-northeast-trending dry valley in the southern Helliwell Hills (Fig. 1). The valley floor is largely covered by moraine debris, with locally restricted exposures of crystalline basement (Rennick Schists and Granite Harbour Intrusives). The flanks of the valley consist mainly of steep-walled cliffs of Jurassic-age dolerite (Ferrar sills) that contain intercalations of Beacon Supergroup deposits with a cumulative total thickness of about 200 m (Collinson *et al.* 1986; Schöner and John 2014). The thickest, lowermost part of these deposits belongs to the Takrouna Formation; an isolated intercalation (locality BVT; 71°55'72.6"S, 161°25'60.1"E; see Schöner and John 2014), exposed just below the northern valley shoulder and separated from the rest of the succession by a ~450-m-thick sill, consists of a *c.* 25-m-thick succession of reddish-weathered sandstone with abundant *Skolithos* burrows. Outcrops of superficially similar deposits also occur on a north-south-trending ridge immediately west of Boggs Valley (locality BVR; 71°55'46.0"S, 161°20'59.1"E) and on top of an isolated, steep-walled mesa of a Ferrar sill still 2 km farther northwest (locality BVM; 71°55'15.9"S, 161°18'47.2"E).

*Area north of Mount Van der Hoeven*.—The extensive, rugged outcrop terrain north of Boggs Valley (Fig. 1) consists mostly of exposures and slope debris of Ferrar Dolerite that locally contain a <100-m-thick intercalation of Beacon Supergroup deposits. We prospected two outcrop areas approximately 2 km north of Mount Van der Hoeven in which these deposits are exposed. The northern one of these (locality MVH; 71°53'25.4"S, 161°25'20.0"E) was sampled and documented during two day-trips; time constraints prevented detailed logging of the section.

*Unnamed ridge in the central Helliwell Hills*.—The outcrop (71°47'33.5"S, 161°22'16.3"E) is a narrow ridge extending southwards from an isolated, unnamed nunatak in the central Helliwell Hills, about half-way between Mount Remington and Mount Bresnahan (Fig. 1). The gently southward-dipping, staircase-like section (section BS) rises from snow cover, exposes a *c.* 165-m-thick section of the Takrouna Formation and overlying reddish-weathered silt- and sandstone, and is capped by a sill. With little time in the field remaining, only the top 50 m of the section could be logged; the entire lower part of

ACCEPTED MANUSCRIPT

Downloaded from http://jgs.lyellcollection.org/ at Universitats- und Landesbibliothek Munster on September 16, 2020

the succession was only briefly investigated, sampled, and documented. Thicknesses for the lower part of this section were estimated from outcrop and aerial photographs. Personal communication suggests that this section may have been logged before (Walker pers. comm. 1982 *in* Collinson *et al.* 1986), but no published records exist.

*Helliwell Hills campsite sections*.—Flat-lying Beacon Supergroup deposits are widely exposed along the flanks surrounding an unnamed mesa 3 km east of Dziura Nunatak in the northernmost outcrop area of the Helliwell Hills (Fig. 1). The mesa is the highest elevation in the study area; its peak is a characteristic flat-topped inselberg of Ferrar Dolerite bounded on all sides by more-or-less steep-walled cliffs about 50 m high. The field campsite was installed on flat moraine debris on the valley floor east of the mesa (71°43'58.3"S, 161°22'40.9"E, 1012 m a.s.l.). A composite profile of the sedimentary succession was reconstructed based on individual sections logged from the lowest part of the succession west of the campsite (section HCCL), up the southeastern slopes of the mesa (section HCSE) and onto thin remnants of sedimentary deposits on top of the mesa-forming sill (section HCtop). Further outcrops occur on the slopes all along the perimeter of the mesa (sectors HCNW and HCNE) and some 900 m south-southeast towards the adjacent hillside (sector HCS) (see Fig. S2).

### *Macrophotography*

Images of macrofossils were taken either in the field using a Nikon D7100 digital SLR camera equipped with an AF-S Nikkor 18–200 mm lens, or in the studio using a repro-stand set-up with a Canon EOS 7D digital SLR camera equipped with a Canon EFS 60 mm macro-lens. Samples of silicified wood and peat were photographed under immersion in plain water in order to increase contrast (Kerp and Bomfleur 2011).

### *Petrography and geochemistry*

We selected seven sandstone samples for point-counter analysis on the basis of their grain size and limited recrystallization, ascertained from examination of standard petrographic thin sections (unstained, without cover slip). The ≥63-µm grain-size population of quartz, feldspar and lithic fragments were point-counted (*c.* 400 per thin-section) following the Gazzi-Dickinson method (Ingersoll *et al.* 1984). Framework modes of the analyzed samples were plotted in the QFL (total quartz-feldspar-lithic fragments) and QmFLt (monocrystalline quartz-feldspar-total lithic fragments) ternary diagrams with discrimination fields after Dickinson *et al.* (1983). Three additional

ACCEPTED MANUSCRIPT

Downloaded from http://jgs.lyellcollection.org/ at Universitats- und Landesbibliothek Munster on September 16, 2020

samples (NVL1116, NVL116, and NVL216) were analysed at the German Federal Institute for Geosciences and Natural Resources (Bundesanstalt für Geowissenschaften und Rohstoffe, BGR), Hannover, for petrography, for qualitative mineralogical and bulk-rock geochemical composition (Supplementary Data File, Figs S4, S5, and S7).

### *Palynology*

Twenty palynological samples from across four sections in the Helliwell Hills area were processed following standard protocols (Supplementary Data File). Sample preparations were analysed with a Leica Diaplan microscope with Nomarski interference contrast. Photomicrographs were taken with a Nikon DS-5M digital camera; all specimen illustrations are composite micrographs, each being merged manually from several individual images taken at different focal planes in order to enhance sharpness (Bercovici *et al.* 2009; Kerp and Bomfleur 2011).

Palynological and most lithological samples and slides are housed in the Forschungsstelle für Paläobotanik at the Institut für Geologie und Paläontologie, Westfälische Wilhelms-Universität Münster, Germany; three lithological samples (NVL1116, NVL116, and NVL216) and corresponding thin sections are housed at the German Federal Institute for Geosciences and Natural Resources (Bundesanstalt für Geowissenschaften und Rohstoffe, BGR, Hannover).

## Stratigraphic revision

In the Helliwell Hills, the Permian Takrouna Formation (Fig. S1) is overlain by previously unrecognized sedimentary deposits. Sections in the area around Mount Van der Hoeven immediately north of Boggs Valley expose the basal part of a new stratigraphic unit described here for the first time: the Van der Hoeven Formation (at least 115 m thick). This mainly reddish-weathered siliciclastic sandstone and non-carbonaceous mudstone unit (Fig. 2) rests on top of the Takrouna Formation; apart from containing a diverse suite of continental trace fossils, the Van der Hoeven Formation is barren of macrofossils (Fig. 2). In the northern Helliwell Hills, the Van der Hoeven Formation is overlain by another new stratigraphic unit described here, the Helliwell Formation, (235 m thick) that is dominated by recessive, commonly carbonaceous mudstone with cliff-forming intercalations of greenish, medium-grained sandstone (Figs 3, S2, and S4). The Helliwell Formation contains thin coal seams and is rich in plant

ACCEPTED MANUSCRIPT

Downloaded from http://jgs.lyellcollection.org/ at Universitats- und Landesbibliothek Munster on September 16, 2020

fossils, including compression fossils (e.g., *Dicroidium* fronds and *Heidiphyllum* leaves) as well as silicified wood (*Kykloxylon* sp., *Agathoxylon* sp., and a *Woodworthia*-like axis) and silicified peat with anatomically preserved plant remains (Fig. 4). Close to the top of the Helliwells Hills campsite section, the Helliwell Formation is erosively overlain by a succession of conglomerate and garnet-rich pebbly sandstone (Fig. S3) similar in appearance to the basal parts of the Section Peak Formation farther south (see Collinson *et al.* 1986; Schöner *et al.* 2011).

Petrographic analyses and field interpretation indicates that the sandstone types of the previously unrecognized stratigraphic units are readily distinguishable based on characteristic components (Figs 5 and S4): sandstone samples from the Van der Hoeven Formation are overall quartz-rich and can be classified as quartzose to subarkosic arenites; those from the Helliwell Formation are, by contrast, relatively quartz-poor (lithic subarkose to arkosic litharenites) with a high proportion of volcaniclastic detritus, including primarily euhedral feldspar and volcanic lithic fragments as well as abundant zeolites (Supplementary Data File, Fig. S5). The single sample from the Section Peak Formation (HCSE12) is again subarkosic, and further characterized by abundant garnet in the form of macroscopically visible lag layers (Figs 5, S3b, and S4).

Out of twenty mudstone samples processed for palynological analysis and palynostratigraphic age assessment, eight turned out barren, six yielded a low content of palynomorphs insufficiently preserved for identification, and six yielded moderately to well-preserved palynomorph assemblages with sufficient identifiable taxa to enable biostratigraphic age assessment (Fig. 6).

***Beacon Supergroup (Barrett 1970)***

***Victoria Group (Harrington 1965)***

***Takrouna Formation (Dow and Neall 1974)***

Sections of the Takrouna Formation in Boggs Valley and in the Morozumi Range to the east (see Schöner and John 2014) were surveyed and sampled during brief helicopter visits; an additional section comprising the top ~140 m of the Takrouna Formation is exposed at the BS section in the central Helliwell Hills (Figs 1 and S1). Here, the formation consists of three successive facies associations: a lower association (unit 1, *c.* 30 m thick) dominated by trough-cross-bedded, medium- to coarse-grained pebbly

ACCEPTED MANUSCRIPT

Downloaded from http://jgs.lyellcollection.org/ at Universitats- und Landesbibliothek Munster on September 16, 2020

sandstone and conglomerate; a middle association (unit 2, *c.* 65 m thick) consisting of heterolithic sandstone, ripple-laminated fine-grained sand- and siltstone, and carbonaceous mudstone (Fig. S1b); and a third association (unit 3, *c*. 45 m thick) of fining-upward sequences of sandstone, rooted siltstone, and coal-bearing fine-grained deposits (Fig. 2a). Throughout the section, finer-grained deposits are rich in plant detritus and macrofossils typical of the Permian of Gondwana, including *Glossopteris* (Fig. S1c), *Gangamopteris*, and *Vertebraria* (Fig. S1d). A mudstone sample from the top of the Takrouna Formation (BS04, 12 m below the base of the overlying Van der Hoeven Formation) yielded a palynomorph assemblage that is dominated by taeniate-bisaccate glossopterid pollen (Fig. 6a–d) with additional occurrences of *Praecolpatites sinuosus* (Fig. 6e), *Marsupipollenites triradiatus* (Fig. 6f), and cheilocardioid spores, including *Granulatisporites trisinus*, *Dulhuntyispora dulhuntyi* (Fig. 6g), *D. parvithola* (Fig. 6h), and *D*. sp. cf. *D. stellata.* The latter genus—a key index form for the middle to upper Permian palynostratigraphy of Australia (Kemp *et al*. 1977; Price 1997)—is here reported and illustrated from Antarctica for the first time (see Playford 1990; Farabee *et al*. 1991). Together, the taxon composition of the recovered assemblages enables correlation with the late Permian Antarctic *Praecolpatites* zone of Playford (1990), with the late Permian Australian Stage 5/Unit VII of Kemp *et al.* (1977), and with the equivalent upper part of unit APP5 of Price (1997). Our data thus confirm that the age of the Takrouna Formation ranges into the Lopingian (late Permian).

***Van der Hoeven Formation (new stratigraphic unit)***

*Definition*.—We propose the name Van der Hoeven Formation for the 115+-m-thick succession of reddish-weathered, mainly medium- to coarse-grained siliciclastic sandstone in the lower Rennick Glacier area, northern Victoria Land, based on sections in the southern Helliwell Hills that are characterized by (1) common, sheet-like, heterogeneous sandstone bodies with tabular cross bedding (Fig. 2f); (2) general lack of plant macrofossils, coal or carbonaceous mudstone; (3) conglomeratic scour fills containing mainly extraclasts or intraclasts of non-carbonaceous mudstone; and (4) local abundance of trace fossils representing the *Skolithos* ichnofacies, the *Scoyenia* ichnofacies, indistinct (i.e., non-*Vertebraria*) root traces in palaeosols, and mass occurrences of *Cylindricum*-type sand plugs penetrating intraclasts of conglomeratic scour-fill bases (Fig. 2g–i).

ACCEPTED MANUSCRIPT

Downloaded from http://jgs.lyellcollection.org/ at Universitats- und Landesbibliothek Munster on September 16, 2020

*Etymology*.—After Mount Van der Hoeven, the highest peak in the area immediately north of Boggs Valley, where the formation is extensively exposed on plateaus and in cliff faces. Mount Van der Hoeven is named in honour of Dutch seismologist Frans G. Van der Hoeven, leader of the 1959–1960 Victoria Land Traverse expedition.

*Type section (provisional)*.—An exposure with a total thickness of about 50 m along the southern and eastern flank of a small unnamed knob 1.5 km north of Mount Van der Hoeven (section MVH; 71°53'25.4"S, 161°25'20.0"E; Fig. 2c); here, the base of the section is covered in slope debris and the top of the section is capped by a Ferrar sill.

*Additional sections*.—The lower boundary and basal 15 m of the formation are exposed on an unnamed ridge informally referred to as 'Schöner Rücken' (section BS) in the central Helliwell Hills (Figs 3a and b, S1a). In the southern Helliwell Hills, the formation crops out above a narrow ledge below the northern valley shoulder of Boggs Valley itself (section BVT), occurs at an isolated ridge (section BVR) and isolated mesa (section BVM) a few kilometres west of the head of Boggs Valley, and is widely exposed in cliff faces on the rugged plateau north of Boggs Valley. In this entire area, sections of the formation occur sandwiched between thick Ferrar sills; in most places, the finer-grained and recessive basal part of the formation is covered in slope debris, leaving mainly the cliff-forming, sandstone-dominated upper part of the formation well exposed. Similarly, in the northern Helliwell Hills, a 65-m-thick section of the upper part of the formation forms the lowest cliff exposure (section HCCL) along the eastern flank of an unnamed mesa west of our campsite (Figs 2f, 3, and S2).

Possible further occurrences that require additional study include the successions of lighter-coloured sandstone beds that rest on top of sills in the Morozumi Range (Dow and Neall 1974); the isolated outcrops west of Moawhango Névé and around Smith's Bench (Freyberg Mountains) characterized by quartzose, commonly tabular-cross-bedded sandstones with mass occurrences of vertical *Skolithos* burrows and other trace fossils (Hammer and Zawiskie 1982; Zawiskie *et al*. 1983; Collinson *et al.* 1986; John 2014; Schöner and John 2014); and an 8-m-thick section of sandstone with abundant *Skolithos* burrows and invertebrate trails in the southern Retreat Hills (John 2014; Schöner and John 2014) (see Fig. 1). Sedimentary deposits at these latter occurrences have been previously assigned to the Takrouna Formation (Hammer and Zawiskie 1982; Zawiskie *et al*. 1983; Collinson *et al.* 1986; John 2014; Schöner and John 2014).

ACCEPTED MANUSCRIPT

Downloaded from http://jgs.lyellcollection.org/ at Universitats- und Landesbibliothek Munster on September 16, 2020

*Topographic map reference*.—Exposures of the formation are so far known to occur only in outcrop areas depicted on topographic map sheet Daniels Range (SR 57-58/14) of the United States Geological Survey Antarctica 1:250000 Reconnaissance Series; possible further occurrences (see above) are depicted on the topographic map sheet Freyberg Mountains (SS 58/60-1) of the same series.

*Thickness.*—115+ m; since no single completely exposed section has been found in the area, this is a composite estimate based on adding a thickness of ~50 m for the usually recessive lower part of the formation, partly exposed at the MVH section (Fig. 2c), to the 65-m thick sandstone-dominated upper part of the formation, measured at the HCCL section (Figs 3 and S2).

*Lower boundary*.—The lower boundary is marked by an abrupt transition at the BS section from an association of variegated sandstone, carbonaceous finer-grained deposits with glossopterid plant fossils (*Glossopteris*, *Gangamopteris*, *Vertebraria*), and coal of the Takrouna Formation (Fig. S1) below to a succession of silty, non-carbonaceous, olive-grey barren mudstone (Fig. 2b) with intercalations of reddish-weathered, quartzose pebbly sandstone. We place the boundary at the base of a 2-m-thick sandstone bed (BS08), as it forms a conspicuous and well-exposed marker within a ~10-m-thick interval of recessive mudstone.

*Upper boundary*.—The upper boundary of the Van der Hoeven Formation is covered in slope debris at the Helliwell Hills campsite SE section (Figs 3 and S1), but is overall marked by a transition from cliff-forming, reddish-weathered sandstone into the ~40-m-thick, slope-forming lower part of the Helliwell Formation that consists mainly of carbonaceous mudstone with thin, lens-shaped bodies of olive-grey silt- and fine-grained sandstone. We provisionally place the boundary half-way between the top of the highest, well-exposed bed of climbing-ripple-laminated sandstone (HCCL10) and the base of the succeeding bench of fine-grained sandstone (HCSE01) 20 m up-section.

*Lithology*.—The base of the formation at the BS section (Figs 7 and S1a) begins with a 2-m-thick, trough-cross-bedded sandstone body (BS08) with a conglomeratic base containing abundant angular quartz pebbles and rare mudstone clasts. It is overlain by a 15-m-thick succession of mainly olive-grey, non-carbonaceous mudstone (Fig. 2b), poorly sorted, ripple-laminated fine-grained sandstone with pebbly to coarse-grained

ACCEPTED MANUSCRIPT

Downloaded from http://jgs.lyellcollection.org/ at Universitats- und Landesbibliothek Munster on September 16, 2020

basal laminae, and a 3-m-thick intercalation of trough-cross-bedded, pebbly quartzose sandstone (Fig. 7).

The only additional exposure of the lower part of the Van der Hoeven Formation that we studied (MVH section; Fig. 2c) is dominated by stacks of metre-scale beds of low-angle inclined, climbing-ripple-laminated fine-grained sandstone, with minor intercalations of thin beds of reddish-weathered, medium- to coarse-grained pebbly sandstone containing abundant angular quartz fragments and olive-green mudstone intraclasts. Near the top of this lower part occurs a conspicuous, 40-cm-thick ferruginized palaeosol horizon containing vertical, non-carbonaceous root traces and thick, nodular concretions up to 15 cm in diameter (Fig. 2d). This lower part of the section is truncated by an erosional surface, and is overlain by an intraclast-rich conglomeratic scour fill followed by a 2-m-thick, laterally continuous bed of tabular-cross-bedded, coarse- to medium-grained heterogeneous sandstone with pebbly basal layers (Fig. 2e).

Exposures at Boggs Valley (BVR, BVM) and in the northern Helliwell Hills (HCCL; Figs 3 and S2) demonstrate that the upper part of the formation consists of an at least 65-m-thick cliff-forming stack of usually 1–2-m-thick, sheet-like beds of reddish-weathered, medium- to coarse-grained, quartzose to subarkosic sandstone exhibiting conspicuous tabular or trough-shaped cross-bedding (Fig. 2f). Recessive finer-grained intercalations in this part typically consist of successions of low-angle inclined, climbing-ripple-laminated beds of grey-greenish, fine-grained, platy sandstone and siltstone.

*Petrography.*—Sandstone samples from the Van der Hoeven Formation can be classified as quartzose, subarkosic, and lithic-subarkosic sandstones (Figs 5 and S4). Sample NVL1116 is a moderately sorted quartzose to subarkosic sandstone with abundant quartz and subordinate feldspar in a light brown-coloured, clayey to highly sericitic matrix. Individual grains are mostly angular to subangular and are typically oriented with their long axes parallel to bedding. Quartz grains are mostly monocrystalline with wavy extinction, inclusion trails, and a variety of inclusions (e.g., rutile, zircon, sillimanite); polycrystalline quartz grains occur rarely. Potassium-feldspar (microcline, orthoclase) and plagioclase are identified by their twinning and, in some grains, strong sericitization. Some grains show deformation twins indicative of crystal-plastic deformation. Lithic fragments are mostly metamorphic and plutonic in origin;

ACCEPTED MANUSCRIPT

Downloaded from http://jgs.lyellcollection.org/ at Universitats- und Landesbibliothek Munster on September 16, 2020

subordinately there are very fine-grained quartzose grains that could be chert fragments or fine-grained silicic volcanic rocks; however, no rock fragments of definite volcanic origin were observed. In addition, the sample contains relatively large white mica and accessory minerals (e.g., zircon, apatite, garnet).

*Macrofossil content*.—Unlike in the underlying Takrouna Formation and overlying Helliwell Formation, no plant macrofossils or animal body fossils have been found in the Van der Hoeven Formation despite intensive search efforts. The formation, however, has yielded a diverse and characteristic suite of trace fossils, including representatives of the typical in-channel *Skolithos* ichnofacies (dominated by vertical invertebrate burrows; e.g., *Skolithos*, *Arenicolites*; Fig. 2g) and the lower-energy, overbank-environment *Scoyenia* ichnofacies with horizontal burrows (e.g., *Scoyenia*, *Planolites*, *Cochlichnus*; Fig. 2j), with abundant small, vertical, sand-filled burrows (*Cylindricum*; Fig. 2h), and with invertebrate trails (*Aulichnites*) and tracks (*Diplichnites*; Fig. 2i).

*Palynology*.—Out of three samples processed, two samples from the base of the formation at the BS section (GXI-BS08) and from the central part of the formation at the type section (GXI-VDH01) have yielded moderately well-preserved palynomorph assemblages; a further sample from an isolated outcrop of the formation at the head of Boggs Valley (BVR) proved barren. The palynomorph assemblages recovered are essentially non-marine; that of the lower sample (GXI-SR08) is dominated by cavate-trilete plant spores, whereas that of the upper sample is dominated by fragments of non-taeniate bisaccate pollen (mainly *Scheuringipollenites*; Fig. 6o). Both samples have yielded the biostratigraphically significant *Limatulasporites* sp. (Fig. 6k), *Retusotriletes nigritellus* (Fig. 6l), *Endosporites papillatus* (Fig. 6m), *Playfordiaspora crenulata* (Fig. 6n), and *Densoisporites* spp. (Fig. 6i), and both contain common to abundant leiosphaerid acritarchs and the putative fungal or algal remain *Reduviasporonites catenulatus* (Fig. 6q).

*Biostratigraphic age assessment*.—Palynomorph assemblages from the base and the central part of the Van der Hoeven Formation are overall typical of the Australian *Playfordiaspora crenulata* zone of Helby *et al.* (1987) and equivalent unit APP6 of Price *et al.* (1997); compared to recent revisions of the Australian palynostratigraphic zonation in the Sydney Basin (Fielding *et al.* 2019; Mays *et al*. 2020), the occurrence of *Playfordiaspora crenulata* and of *Limatulasporites* sp.—there typical for the succeeding

ACCEPTED MANUSCRIPT

Downloaded from http://jgs.lyellcollection.org/ at Universitats- und Landesbibliothek Munster on September 16, 2020

unit APT1 (Mays *et al.* 2020)—indicates an assignment to the upper part of this zoneand therefore an earliest Triassic age for this part of the Van der Hoeven Formation. The age range of the Van der Hoeven Formation is further bracketed by biostratigraphic data from the formations below and above. Macro- and microfossils from the underlying Takrouna Formation indicate a late Permian age for deposits *c.* 12 m below the base of the Van der Hoeven Formation (see above). From the overlying Helliwell Hills Formation, the closest biostratigraphic indicator is a palynomorph assemblage from about 25 m above the top of the Van der Hoeven Formation, which indicates a Middle Triassic age for that part of the Helliwell Formation (see below). Hence, we consider the Van der Hoeven Formation to be essentially Early Triassic in age.

*Palaeoenvironment*.—The Van der Hoeven Formation is interpreted as the deposits of a low-gradient, sand-dominated braided-river plain. The sandstone composition (Figs 5 and S6) indicates a cratonic source of metamorphic and plutonic basement, probably westward on the East Antarctic craton. Floodplain deposits consist mostly of climbing-ripple-laminated silt- and fine-grained sandstone. Occurrences of primary mudstones are rare and restricted to the lowermost part of the formation; higher up-section, mudstone occurs only secondarily in the form of intraclasts deposited in the conglomeratic scour fills of channel bases. All mudstones are essentially non-carbonaceous and coal deposits are absent. Therefore, floodplain environments are inferred to have been better-drained and climatic conditions possibly drier, even though evidence for seasonal aridity, such as mudcrack horizons or primary redbed deposits as in the Lower Triassic of the central Transantarctic Mountains (e.g., Retallack and Krull 1999; Collinson *et al.* 2006) is absent. Plant macrofossils are lacking, but rooted palaeosols provide evidence of presumably low-growing vegetation cover. The recovered palynomorph assemblages contain a large proportion of cavate-trilete plant spores produced by herbaceous lycophytes (see, e.g., Balme 1995). Pioneering communities dominated by such 'disaster taxa' are thought to have proliferated in the wake of the end-Permian biotic crisis (e.g., Looy *et al*. 2001).

### *Helliwell Formation (new stratigraphic unit)*

*Definition*.—We propose the name Helliwell Formation for a 235-m-thick sedimentary succession in the lower Rennick Glacier area, northern Victoria Land, based on a composite section in the northern Helliwell Hills that is characterized by (1) a high

ACCEPTED MANUSCRIPT

Downloaded from http://jgs.lyellcollection.org/ at Universitats- und Landesbibliothek Munster on September 16, 2020

proportion of slope-forming, fine-grained sandstone and mudstone with intercalated coal seams; (2) cliff-forming intercalations of greenish-weathered, homogeneous fine- to medium-grained, typically trough-cross-bedded, volcaniclastic sandstone; (3) scour surfaces overlain by conglomeratic basal layers containing mainly intraclasts of carbonaceous mudstone and coal; and (4) common plant fossils, including leaf adpressions, coalified or silicified wood, and silicified peat.

*Etymology*.—After the Helliwell Hills, where type and additional sections of the formation have been studied. The Helliwell Hills are named in honour of Robert A. Helliwell (1920–2011), U.S. American electrical engineer at Stanford University affiliated with the U.S. Antarctic Research Program.

*Type section*.—A 235-m-thick section up the southeastern slope of an unnamed inselberg in the northern Helliwell Hills (section HCSE: 71°44'02.0"S, 161°21'36.1"E; Figs 3, 8, and S2), *c.* 3 km east of Dziura Nunatak.

*Additional sections*.—So far only known to crop out in the northern Helliwell Hills along the hill slopes in the immediate vicinity of the PNRA/GANOVEX XI/KAGEX III camp site.

*Topographic map reference*.—Exposures of the formation are so far known to occur exclusively in outcrop areas depicted on topographic map sheet Daniels Range (SR 57-58/14) of the United States Geological Survey Antarctica 1:250000 Reconnaissance Series.

*Thickness*.—~235 m.

*Lower boundary.*—Not observed; occurs within a 25-m-thick interval of slope debris between the top (bed HCCL10) of the underlying cliff-forming sandstone of the Van der Hoeven Formation and the base of a thin interval of carbonaceous silt- to fine-grained sandstone (bed HCSE01o; Fig. 4a) characterized by symmetrical ripples, mud drapes, finely disseminated plant debris, and a well-preserved microflora of Middle Triassic age (see below).

*Upper boundary.*—The top of the formation is separated from the disconformably overlying basal conglomeratic sandstones of the Section Peak Formation (see below) by an erosional surface (Fig. 4h) with a local relief of 2+ m, observed over a distance of

ACCEPTED MANUSCRIPT

Downloaded from http://jgs.lyellcollection.org/ at Universitats- und Landesbibliothek Munster on September 16, 2020

about 100 m along a continuous exposure immediately underneath the plateau-forming dolerite sill at the type section.

*Lithology*.—The Helliwell Formation is overall dominated by fine-grained, recessive overbank deposits (Figs 3 and 4d); where exposed, these consist mainly of dark-grey to almost black, commonly root-bearing carbonaceous mudstones, locally with thin coal seams and cm- to dm-thick intercalations of greenish, ripple-laminated silt- and fine-grained sandstone (Fig. 4d). Weathered slope surfaces within these fine-grained successions commonly bear mass accumulations of oblate, whitish, somewhat powdery concretions *c.* 2–3 cm in diameter that we interpret as pustular zeolite concretions. Two major cliff-forming intercalations of fine- to medium-grained volcaniclastic sandstone, 55 m and 27 m thick respectively, occur in the lower and in the upper part of the formation (Figs 3, 4b, and 8). Grainsizes within the sandstone beds are homogeneous to such degree that many sandstone bodies appear almost massive, with only faint indication of internal stratification. Trough-cross-bedded scour fills with abundant coalified wood and intraclasts of coal and coaly mudstone (Fig. 4b) are common; some of these are so rich in intraclasts of carbonaceous mudstone that they form clast-supported conglomerates (Fig. 4c).

*Petrography.*—Sandstone samples from the Helliwell Formation overall can be characterized as fine- to medium-grained, moderately sorted lithic subarkoses to feldspathic litharenites (Figs 5 and S4). Samples NVL116 and NVL216 contain accessory subhedral zircon, apatite, amphibole, and tourmaline. Quartz is typically monocrystalline with no or only very weak wavy extinction, and with angular shapes locally showing corrosion and dissolution embayments indicative of a volcanic origin. Polycrystalline quartz is subordinate. Feldspars are mostly plagioclase with a minor amount of K-feldspar, which is often sericitized. Some individual feldspar grains occur as euhedral laths with no or only very weak wavy extinction, with either polysynthetic (plagioclase) or—rarely—Karlsbad twinning, the latter possibly indicative of sanidine crystals derived from volcanic rocks. Lithic fragments consist of clastic (partly low-grade metamorphic) sedimentary rocks, volcanic rocks with microphenocrysts of feldspar in a fine-grained diffuse matrix, and fine-grained quartzose fragments, which could be cherts or fine-grained volcanic rocks due to common chloritization of these grains. Unlike in the sandstones of the underlying Van der Hoeven Formation, clear high-grade

ACCEPTED MANUSCRIPT

Downloaded from http://jgs.lyellcollection.org/ at Universitats- und Landesbibliothek Munster on September 16, 2020

metamorphic rock fragments and polycrystalline quartz are only a minor component, as are quartz-feldspar aggregates of plutonic origin.

*Macrofossil content*.—Mudstones throughout the formation have yielded sparse plant adpression fossils, including leafy sphenophyte stems (*Schizoneura*), lycopsid sporophylls (*Lepacyclotes* sp.; Fig. 4e), and fragments of *Dicroidium* fronds. A dark mudstone bed (HCSE10) near the top of the unit has yielded a rich assemblage of compression fossils dominated by the conifer leaf *Heidiphyllum elongatum* (Fig. 4f), with rare additional occurrences of seed-fern foliage (*Linguifolium tenison-woodsii* and *Dejerseya lobata*) and small bivalved invertebrates . Channel fills of medium-grained sandstone typically contain abundant fragments of coalified wood. Surface rubble in the lower half of the slopes of the type section contains abundant pieces of silicified wood (Fig. 5g) and blocks of silicified peat with structurally preserved plant remains , including osmundaceous fern rhizomes. A slab of fine-grained sandstone collected from the surface layer in the central part of the type section has yielded an isolated tetrapod footprint that was tentatively assigned to the ichnogenus *Procolophonichnium* (Mörs *et al.* 2019).

*Palynology*.—Out of eleven samples processed, three samples from the base (HCSE01o), the central part (HCSE08l), and the top (HCSE10) of the formation have yielded palynomorph assemblages sufficiently well-preserved to enable palynostratigraphic age assessment. Palynomorph content of all samples is dominated by bisaccate non-taeniate pollen, including *Alisporites australis* (Fig. 6w) and *Platysaccus queenslandii* (Fig. 6x). Sample HCSE01 further contains common cavate-trilete spores (*Densoisporites* spp. and *Lundbladispora* spp.; Fig. 6t), various species of *Aratrisporites* (including *A. tenuispinosus* and *A. fischeri*: Fig. 6r and s) and the biostratigraphically significant *Staurosaccites quadrifidus* (Fig. 6v), and *Ephedripites steevesii* (Fig. 6u). Spore assemblages of sample HCSE08l contain abundant cingulate bryophyte spores (including *Rogalskaisporites cicatricosus*, *Annulispora folliculosa*, and *A. microannulata*; Fig. 6aa–ac), and the biostratigraphically significant *Limbosporites denmeadii* (Fig. 6y) and *Craterisporites rotundus* (Fig. 6z), whereas sample HCSE10 contains *Annulispora folliculosa* (Fig. 6ab) as well as *Enzonalasporites densus*.

*Biostratigraphic age assessment*.—The HCSE01o palynomorph assemblage from the lower part of the formation can be correlated with subzone B of the informal Antarctic

ACCEPTED MANUSCRIPT

Downloaded from http://jgs.lyellcollection.org/ at Universitats- und Landesbibliothek Munster on September 16, 2020

*Alisporites* zone (Kyle 1977; Kyle and Schopf 1982) and with the Australian *Staurosaccites quadrifidus* Zone of Helby *et al.* (1987) and the equivalent upper part of unit APT3 of Price (1997). Those from the middle (HCSE08l) and upper (HCSE10) portions of the Helliwell Formation can be correlated with the subzone C of the Antarctic *Alisporites* zone (Kyle 1977; Kyle and Schopf 1982) and with the Australian-New Zealand *Annulispora folliculosa* Zone of de Jersey and Raine (1990; see Bomfleur *et al*. 2014a) and the equivalent unit APP4 of Price (1997). The age of the Helliwell Formation is thus estimated to be Middle Triassic to middle Late Triassic (Norian). This assignment agrees well with the identification of *Heidiphyllum*, *Dicroidium*, *Linguifolium*, and *Dejerseya* leaves, which all are characteristic plant macrofossils in the Middle and Upper Triassic of high-latitude Gondwana (e.g., Anderson and Anderson, 1983, 1989), including Antarctica (e.g., Bomfleur *et al.* 2011; Escapa *et al.* 2011; Oh *et al*. 2016).

*Palaeoenvironment*.—The high proportion of fine-grained overbank deposits in the Helliwell Formation is typical of a meandering-stream system with extensive floodplains. Intercalated cliff-forming channel sandstones, however, lack the typical point-bar lateral accretion sets. They are instead characterized by stacks of scour-based, trough-cross-bedded sandstone bodies typical of a sand-dominated braided-stream system. In this respect, the fluvial depositional system is similar to the 'transitional facies' inferred for parts of the Fremouw and Lashly formations in the Transantarctic Mountains and the Cluan and equivalent formations in Tasmania (Collinson *et al*. 1987). The volcaniclastic composition of the sandstones testifies to intense contemporaneous volcanism, indicative of an active continental margin setting for the Middle to Late Triassic. Carbonaceous and rooted overbank deposits, abundant fossil wood, plant compression fossils, coal, and silicified peat together indicate that favourable climatic conditions supported highly productive and locally peat-forming vegetation cover in the floodplain, represented in the upper part of the formation by typical Gondwanan *Heidiphyllum* and *Dicroidium* forests.

### *Section Peak Formation (Collinson et al. 1986)*

Truncated by an up to 2-m-deep scour surface, the top of the Helliwell Formation at the type section is unconformably overlain by a succession of coarse- to medium-grained, light-grey to yellowish quartzose sandstone capped 4 m upsection by a *c*. 50-m-thick dolerite sill (Figs 3, 4h, and S3). The base of this succession consists of an up to c. 1-m-

ACCEPTED MANUSCRIPT

Downloaded from http://jgs.lyellcollection.org/ at Universitats- und Landesbibliothek Munster on September 16, 2020

thick conglomeratic channel fill that contains large, angular to variably rounded quartzitic clasts, coalified wood, and medium-grey mudstone intraclasts (Fig. 4h); a lag layer near the base of the unit attains a pink- to reddish colour due to mass accumulation of sand-sized garnet grains (Fig. S3a). The overlying sandstones appear almost massive due to a rather homogeneous grain size, but differential weathering colours indicate internal trough-cross-bedding. On the planar top of the sill there are local remnants of similar trough-cross-bedded sandstone deposits with a maximum thickness of about 10 meters (Fig. S3c). Bases of cross-bedded units commonly contain intraclasts of medium-grey mudstone (Fig. S3d). One such intraclast was sampled for palynological analysis, but yielded only very few identifiable palynomorphs (Fig. S3e). Common among these are coarsely sculptured, asaccate pollen grains (Fig. 6ad) similar to *Araucariacites* cf. *australis* of Zhang and Grant-Mackie (2001: fig. 25c) and bisaccate non-taeniate pollen grains, including *Podocarpidites*-type pollen with a distinctly granulate cappa (Fig. 6ae); another conspicuous form is a fragmented, large laevigate fern spore with a subtriangular amb and a differentially thickened equatorial cingulum (Fig. 6af) that appears similar to certain spores of Matoniaceae (e.g., *Trilobosporites*, *Matonisporites*, or *Murospora*). The low sample yield and unusual composition of the assemblage likely reflects strong taphonomic and diagenetic biases. Despite the probably skewed composition, and even though the assemblage lacks the typical abundance of cheirolepidiaceous pollen, we tentatively interpret it to indicate an Early Jurassic rather than Late Triassic age for the intraclast (and thus a possibly younger age for the host deposit), since the above-mentioned taxa typically appear in Early Jurassic palynomorph assemblages of Antarctica (see, e.g., Tasch and Lammons 1978; Musumeci *et al.* 2006; Ribecai 2007; Bomfleur *et al*. 2014a) and adjacent regions of Gondwana (see, e.g., de Jersey 1960, 1963; Filatoff 1975; Zhang and Grant-Mackie 2001).

We assign this unit to the Section Peak Formation based on similar field aspect, sandstone composition, bedding features, and prominent content of garnet in the form of macroscopically visible lag layers (see Collinson *et al.* 1986; Schöner *et al.* 2011; Elsner 2013).

## Discussion

### *Correlation of stratigraphic units*

ACCEPTED MANUSCRIPT

Downloaded from http://jgs.lyellcollection.org/ at Universitats- und Landesbibliothek Munster on September 16, 2020

The revised succession of stratigraphic units in the study area (Fig. 9) can be overall well correlated with those from other regions of the Transantarctic Mountains (see Barrett 1981, 1991; Collinson *et al*. 1994; Elliot *et al*. 2017; Goodge 2020) and from Tasmania (e.g., Forsyth 1987; Collinson *et al.* 1990) (Fig. 10). The presence of the characteristic microfloras of the *Praecolpatites* zone of Playford (1990) in the upper part of the Takrouna Formation indicates that deposition was contemporaneous with that of the upper Weller Coal Measures of SVL (see Askin 1997) and with the Buckley Coal Measures, Queen Maud Formation, and upper Mount *Glossopteris* Formation of the central Transantarctic Mountains (see Playford 1990).

The Van der Hoeven and Helliwell formations have no immediately correlative strata anywhere in northern Victoria Land; the nearest outcrops of correlative units occur more than 500 km farther afield, southwards beyond the David Glacier and northwards in Tasmania. The Van der Hoeven Formation can be well correlated with the Feather Sandstone or Feather Conglomerate of southern Victoria Land and with the lower Fremouw Formation in the central Transantarctic Mountains, based on (1) similar quartzose to subarkosic sandstone composition; (2) similar depositional features, including common sheet-like sandstone bodies with planar or trough-shaped cross bedding; (3) similar occurrence of non-carbonaceous mudstone and soil horizons; (4) similar scarcity of plant macrofossils, and notable absence of both *Glossopteris* (typical of the respective underlying units) and *Dicroidium* (typical of the respective overlying units); and (5) similar trace-fossil assemblages (see Barrett 1969; McElroy 1969; Korsch 1974; Ballance 1977; Barrett and Fitzgerald 1985; Fitzgerald and Barrett 1986; Miller and Collinson 1994). Similar sedimentological and lithological features are shared also with unit 2 of the upper Parmeener Supergroup of Tasmania, including the Ross and lower Cluan formations (Forsyth 1987; see Collinson *et al*. 1987).

The Helliwell Formation is correlated with members A to C of the Lashly Formation in southern Victoria Land and with the middle and upper part of the Fremouw Formation, central Transantarctic Mountains, based on (1) high proportion of carbonaceous overbank deposits; (2) homogeneous fine to medium grain size and prominent volcaniclastic component of sandstone intercalations; (3) common occurrence of Middle to Late Triassic plant compression fossils, including *Heidiphyllum*, *Dicroidium*, *Linguifolium*, and *Dejerseya*; and (4) abundant occurrences of silicified peat and wood, including *Kykloxylon* (see Barrett 1969; Korsch 1974; Barrett *et al.* 1986;

ACCEPTED MANUSCRIPT

Downloaded from http://jgs.lyellcollection.org/ at Universitats- und Landesbibliothek Munster on September 16, 2020

Collinson *et al.* 1987, 1994; Bomfleur *et al.* 2011; Escapa *et al.* 2011; Decombeix *et al.* 2014; Oh *et al.* 2016). Likewise similar in lithology and sedimentological features is unit 3 of the upper Parmeener Supergroup in Tasmania (Forsyth 1987), including the upper Cluan, Tiers, and lower Brady formations and equivalents (Collinson *et al.* 1987, Forsyth 1987). The single studied exposure of the Section Peak Formation in the study area probably represents the upper, Jurassic part of the formation, based on the absence of coal, carbonaceous mudstone, or plant macrofossils, and on the similarity to exposures of the upper Section Peak Formation at outcrops west of the upper Rennick Glacier (see Schöner *et al.* 2011). This upper part of the Section Peak Formation is correlative with the lower Hanson Formation of the central Transantarctic Mountains and with unnamed, mixed volcaniclastic-epiclastic deposits in the Convoy Range and Ricker Hills areas of southern Victoria Land (Elliot and Grimes 2011; Unverfärth *et al. in press*). Deposits of similar age and characteristics are thus far unknown from Tasmania.

Altogether, the emended stratigraphic record for the Victoria Group in the lower Rennick Glacier area (Fig. 9) gives a more detailed picture of the basement topography for the Beacon Supergroup in northern Victoria Land (Fig. 10). The Deep Freeze Range and upper Rennick Glacier areas are unique within the Transantarctic Mountains in that Palaeozoic deposits are absent altogether (Barrett 1991; Collinson *et al.* 1994). Instead, the onset of Beacon Supergroup sedimentation began there as late as during the Late Triassic–Early Jurassic. It remains unclear at present whether this diachronicity merely reflects cratonward onlap onto the basin margin (see, e.g., fig. 3.15 of Barrett 1991 and fig. 8 of Collinson *et al.* 1994) or whether it could be due to a basement high that might have separated individual depocenters in the Transantarctic basin system. In this respect, it is important to note that the assumed hiatus consuming the middle to late Late Triassic between the Helliwell and Section Peak formations has no correlative stratigraphic gap farther south, but may possibly occur in the Tasmanian Triassic, as it does across eastern Australia (e.g., Jell 2013).

### *Biostratigraphic implications*

The biostratigraphic age framework for the Victoria Group of the Transantarctic Mountains is poorly resolved. A diverse assemblage of vertebrate fossils occurs in the lower Fremouw Formation, central Transantarctic Mountains (Barrett 1968; Elliot *et al.*

ACCEPTED MANUSCRIPT

Downloaded from http://jgs.lyellcollection.org/ at Universitats- und Landesbibliothek Munster on September 16, 2020

1970; Hammer 1990; Sidor *et al.* 2008; Peecook *et al.* 2019); the high degree of endemism and the peculiar co-occurrence of taxa that are elsewhere typical of either older or younger strata, however, render the biostratigraphic significance of this fauna inconclusive (Fröbisch *et al.* 2010; Peecook *et al.* 2019). Throughout the Transantarctic Mountains, plant macrofossils are locally abundant (see, e.g., Escapa *et al.* 2011, Cantrill and Poole 2012), but these offer only coarse temporal resolution. Moreover, puzzling outlier occurrences of characteristic plant fossils in younger-than-expected deposits—such as *Glossopteris* leaves in presumably lowermost Triassic strata (e.g., Collinson *et al.* 2006; Elliot *et al.* 2017) and *Dicroidium* fronds in the Lower Jurassic (Bomfleur *et al.* 2018)—cast doubt on the accuracy and precision of plant-macrofossil biostratigraphy at high palaeolatitudes. Pollen-and-spore assemblages can mitigate such effects via many-times greater base data, but altogether, still only few and rather patchy occurrences of microfloras have been reported from the Victoria Group of the Transantarctic Mountains (Helby and McElroy ; Kyle 1977; Kyle and Fasola 1978; Kyle and Schopf 1982; Farabee *et al.* 1989, 1990, 1991; Masood *et al.* 1994; Bomfleur *et al.* 2014a, b; Cornamusini *et al.* 2017). As a result, evidence for a palynostratigraphic zonation of the Victoria Group has been slow to accumulate (Kyle 1977, Kyle and Schopf 1982, Playford 1990, Farabee *et al.* 1990); until now, this age framework has significant gaps, temporal resolution is rather low, and comparisons with the well-calibrated Australian zonation are hampered by the seeming absence of index taxa (e.g., Playford 1990).

The results of our palynological analyses are promising in that they contribute to fill these gaps. Our first illustrated record of *Dulhuntyispora*, a key index taxon in the middle and upper Permian palynostratigraphic zonation of Australia, provides supporting evidence to confirm earlier hypotheses that the Antarctic *Praecolpatites* zone of Playford (1990) can be correlated with the Australian Stage 5/Unit VII of Kemp *et al.* (1977) and with the equivalent upper part of unit APP5 of Price (1997). This, in consequence, provides further evidence that the age spans of the Takrouna Formation and correlative formations farther south do range into the Lopingian (late Permian) and are not restricted to early to middle Permian, as suspected earlier (e.g., Kyle 1977, Kyle and Schopf 1982; Collinson *et al.* 1994). We further present the first recovery of biostratigraphically informative palynomorph assemblages from the lower part of barren quartzose sandstone and non-carbonaceous mudstone that overlie the *Glossopteris*-bearing coal measures throughout the Transantarctic Mountains (see, e.g.,

ACCEPTED MANUSCRIPT

Downloaded from http://jgs.lyellcollection.org/ at Universitats- und Landesbibliothek Munster on September 16, 2020

Isbell and Askin 1999; Retallack *et al.* 2005); these assemblages now indicate a hitherto undocumented Early Triassic (Induan) age for at least the lower to middle part of these deposits. Finally, an 18-m-thick interval between two successive palynological samples at the BS section apparently represents the time span from late Permian (Lopingian) to earliest Triassic (Induan). Although the precise time span consumed by the erosional disconformity at the base of the Van der Hoeven Formation is unclear at present, this age bracket leaves a distinct possibility that the BS section contains a more or less continuous Permian-Triassic boundary section, with a stratigraphic record in Victoria Land much more complete than had previously been suspected (e.g., Kyle 1977, Kyle and Schopf 1982, Isbell and Askin 1999). Within the Transantarctic basin system, palynostratigraphic data approaching similar proximity to the Permian-Triassic boundary have thus far only been known from the central Transantarctic Mountains (McManus *et al*. 2002; Collinson *et al*. 2006). At Graphite Peak, pollen-and-spore assemblages typical of the uppermost Permian or basal Triassic—including abundant *Playfordiaspora crenulata* and possible representatives of *Protohaploxypinus microcorpus* and of *Lunatisporites* sp.—occur ~1 m below the top of the Buckley Formation, indicating that the barren lowermost part of the overlying Fremouw Formation may, there, be entirely Triassic in age (Collinson *et al*. 2006). This assignment would agree well with the earliest Triassic age of the presumably correlative Van der Hoeven Formation reported herein. At Collinson Ridge in the central Transantarctic Mountains, however, a typical Permian glossopterid flora occurs ~36 m above the base of the Fremouw Formation (McManus *et al*. 2002, Collinson *et al*. 2006, Elliot *et al*. 2017). Thus far, this contrast has preferably been interpreted either as a result of uncertainties in detrital-zircon geochronology or as indicating a diachronous formation boundary due to facies progradation (Elliot *et al*. 2017). Alternatively, however, the unusual *Glossopteris* assemblage from Collinson Ridge might represent a rare relict flora of typical Permian vegetation elements that survived in high-latitude refugia into the Early Triassic. There is increasing evidence for similar younger-than-expected outlier occurrences also in several other plant groups, which appears to reveal such survival in high-latitude refugia as a common phenomenon in plant evolution (Bomfleur *et al*. 2018).

## Summary and Conclusions

ACCEPTED MANUSCRIPT

Downloaded from http://jgs.lyellcollection.org/ at Universitats- und Landesbibliothek Munster on September 16, 2020

We present a comprehensive revision and emendation for the regional stratigraphy in the far north of the Transantarctic basin system (Fig. 9). The description of new Lower Triassic (Van der Hoeven Formation) and Middle to Upper Triassic (Helliwell Formation) stratigraphic units and recognition of presumably Lower Jurassic deposits (Section Peak Formation) in this area provide important tie-points for correlating regional stratigraphic units of the Beacon Supergroup across the Transantarctic basin system (Fig. 10). The nearest outcrops of correlative stratigraphic units occur in the Allan Hills, more than 500 km farther south. Moreover, our data promise to enable a more detailed evaluation of the link to coeval sedimentary successions of the Tasmania Basin, whose precise relationship with the Transantarctic basin system remains unclear (Collinson *et al.* 1987, 1990). In general, the dramatic changes in dominant lithologies, composition, bedding features, and fossil content from the Permian into the Upper Triassic and Lower Jurassic appear remarkably similar to those documented elsewhere in the Transantarctic Mountains: from heterolithic sandstones and *Glossopteris*-bearing coal measures in the upper Permian (Takrouna Formation), through barren Lower Triassic quartzose sandstones reflecting erosion of a cratonic source (Van der Hoeven Formation), to arc-fed volcaniclastic sandstones, mudstones and coals associated with typical elements of the Middle to Late Triassic *Dicroidium* flora (Helliwell Formation). Of special importance is the discovery of a potentially continuous section spanning the transition from upper APP5 to APP6 palynofloras—the interval that is currently thought to mark the terrestrial expression of the end-Permian mass extinction (Fielding *et al.* 2019; Mays *et al.* 2020). Future high-resolution sampling of this section will hopefully allow a detailed reconstruction of high-latitude vegetation dynamics across this critical interval in Earth History.

ACCEPTED MANUSCRIPT

## Acknowledgments

We thank the Federal Institute for Geosciences and Natural Resources (Bundesanstalt für Geowissenschaften und Rohstoffe–BGR, Hannover, Germany) for the invitation to join the expedition and for generous logistical support in the field, and the Italian Antarctic Research Programme (PNRA) for generous support and hospitality at Mario Zucchelli Station and onboard the *Italica*. We thank the GANOVEX XI team for productive and enjoyable field work; our helicopter staff Gareth I. McCurdy, Dion Parker, Matthew Walton and Philip Wesley (Helicopters New Zealand, Nelson) and our mountain guides

Downloaded from http://jgs.lyellcollection.org/ at Universitats- und Landesbibliothek Munster on September 16, 2020

Mike Atkinson and Maurice Conway for great support; David H. Elliot (Columbus, OH) and Chris Mays (Stockholm) for valuable comments and suggestions on an earlier version of our manuscript; Simon Schneider (Cambridge), Jörg W. Schneider (Freiberg, Germany), Frank Scholze (Darmstadt, Germany), and Robert Schöner (Celle, Germany) for helpful discussion; the DigitalGlobe Foundation for providing World View-2 satellite images (Fig. S2); Michelle Dow and Peter Barrett (Antarctic Research Centre, Wellington) for kind assistance with archive search; and Ashleigh van Smeerdijk Hood (Melbourne) for editorial handling.

## Funding

Financial support has been provided by the Swedish Research Council (VR grant 2014-5232 to B.B.), the German Research Foundation (DFG grant BO3131/1-1, Emmy Noether Programme 'Latitudinal Patterns in Plant Evolution' to B.B.), the Italian National Antarctic Research Programme (PNRA projects PNRA_2013/AZ2.02 and PNRA_2016_0040-REGGAE to L.C.), and the Korea Polar Research Institute (KOPRI project PE20200). Technical support has been provided by the Alfred Wegener Institut, Helmholtz-Zentrum für Polar- und Meeresforschung (AWI, Bremerhaven) and by the Swedish Polar Research Secretariat (SPFS, Stockholm).

## Appendix

A Supplementary Data File containing supplementary information, figures S1–S7, and additional references is available at […]

## References

Anderson, J.M. and Anderson, H.M. 1983. *Palaeoflora of southern Africa: Molteno Formation. Vol. 1, Part 1. Introduction/ Part 2. Dicroidium*. A.A. Balkema, Rotterdam.

Anderson, J.M. and Anderson, H.M. 1989. *Palaeoflora of southern Africa: Molteno Formation. Vol. 2. Gymnosperms, excluding Dicroidium*. A.A. Balkema, Rotterdam.

Askin, R. A. 1997. Permian palynomorphs from southern Victoria Land, Antarctica. *Antarctic Journal of the United States*, **30**, 47–48.

Ballance, P.F. 1977. The Beacon Supergroup in the Allan Hills, central Victoria Land, Antarctica. *New Zealand Journal of Geology and Geophysics*, **20**, 1003–1116.

Balme, B.E. 1995. Fossil in situ spores and pollen grains: an annotated catalogue. *Review of Palaeobotany and Palynology*, **87**, 81-323.

Barret, P.J., Baillie R.J. and Colbert E.H. 1968. Triassic Amphibian from Antarctica. *Science*, **161**, 460-462.

ACCEPTED MANUSCRIPT

Downloaded from http://jgs.lyellcollection.org/ at Universitats- und Landesbibliothek Munster on September 16, 2020

Barrett, P.J. 1969. Stratigraphy and petrology of the mainly fluviatile Permian and Triassic Beacon rocks, Beardmore Glacier area, Antarctica. Institute of Polar Studies, Report No. 34. The Ohio State University Research Foundation, Columbus.

Barrett, P.J. 1981. History of the Ross Sea region during the deposition of the Beacon Supergroup 400 - 180 million years ago. *Journal of the Royal Society of New Zealand*, **11**, 447-458.

Barrett, P.J. 1991. The Devonian to Jurassic Beacon Supergroup of the Transantarctic Mountains and correlatives in other parts of Antarctica. *In* Tingey, R.J., *ed. The Geology of Antarctica*. Oxford: Clarendon Press, 120–152.

Barrett, P.J. and Fitzgerald, P.G. 1985. Deposition of the lower Feather Conglomerate, Permian braided river deposits in southern Victoria Land, Antarctica, with notes on the regional paleogeography. *Sedimentary Geology*, **45**, 189–208.

Barrett, P.J., Elliot, D.H. and Lindsay, J.F. 1986. The Beacon Supergroup (Devonian–Triassic) and Ferrar Group (Jurassic) in the Beardmore Glacier area, Antarctica. *In*: Turner, M.D. and Splettstoesser, J.E. (eds) Geology of the Central Transantarctic Mountains. *American Geophysical Union, Antarctic Research Series*, **36**, 339–428.

Bercovici, A., Hadley, A. and Villanueva-Amadoz, U. 2009. Improving depth of field resolution for palynological photomicrography. *Palaeontologia Electronica*, **12** (2), 12 pp.

Bomfleur, B., Taylor, E.L. *et al*. 2011. Systematics and paleoecology of a new peltaspermalean seed fern from the Triassic Polar vegetation of Gondwana. *International Journal of Plant Sciences*, **172**, 807–835.

Bomfleur, B., Schöner, R. *et al*. 2014a. From the Transantarctic Basin to the Ferrar Large Igneous Province—New palynostratigraphic age constraints for Triassic–Jurassic sedimentation and magmatism in East Antarctica. *Review of Palaeobotany and Palynology*, **207**, 18–37.

Bomfleur, B., Schöner, R., *et al*. 2014b. New Palaeozoic deposits of the Victoria Group in the Eisenhower Range, northern Victoria Land, Antarctica. *Antarctic Science*, **26**, 277–278.

Bomfleur, B., Blomenkemper P. *et al.* 2018. Polar regions of the Mesozoic–Paleogene greenhouse world as refugia for relict plant groups. *In*: Krings, M., Harper, C.J. *et al*. (eds) *Transformative Paleobotany*. Academic Press, 593-611.

Borchgrevink, C.E. 1901. First on the Antarctic Continent, Being an Account of the British Antarctic Expedition 1898–1900. Georges Newnes Ltd, London.

Bromfield, K., Burrett, C.F. *et al*. 2007. Jurassic volcaniclastic–basaltic andesite–dolerite sequence in Tasmania: new age constraints for fossil plants from Lune River. *Australian Journal of Earth Sciences*, **54**, 965–974.

Cantrill D.J. and Poole, I. 2012. *The Vegetation of Antarctica through Geological Time*. Cambridge University Press.

Collinson, J.W. and Kemp, N.R. 1983. Permian-Triassic sedimentary sequence in northern Victoria Land, Antarctica. *In*: Oliver, R.L., James, P.R. and Jago, J.B. (eds) *Antarctic Earth Science*. Cambridge University Press, 221–225.

ACCEPTED MANUSCRIPT

Downloaded from http://jgs.lyellcollection.org/ at Universitats- und Landesbibliothek Munster on September 16, 2020

Collinson, J.W., Pennington, D.C. and Kemp, N.R. 1986. Stratigraphy and petrology of Permian and Triassic fluvial deposits in northern Victoria Land, Antarctica. *In*: Stump, E. (ed.) Geological Investigations in Northern Victoria Land. *American Geophysical Union, Antarctic Research Series*, **46**, 211–242.

Collinson, J.W., Kemp, N.R. and Eggert, J.T. 1987. Comparison of the Triassic Gondwana sequences in the Transantarctic Mountains and Tasmania. *In*: McKenzie, G.D. (ed.) Gondwana Six: Stratigraphy, Sedimentology, and Paleontology. *Geophysical Monograph Series*, **41**, 51–61.

Collinson, J.W., Eggert, J.T. and Kemp, N.R. 1990. Triassic sandstone petrology of Tasmania: evidence for a Tasmania-Transantarctic Basin. *Papers and Proceedings of the Royal Society of Tasmania*, **124**, 61–75.

Collinson, J.W., Isbell, J.L *et al*. 1994. Permian-Triassic Transantarctic basin. *In*: Veevers, J.J. and Powell, C.M. (eds) *Permian-Triassic Pangean Basins and Foldbelts along the Panthalassan Margin of Gondwanaland*. Geological Society of America Memoir, **184**, 173–222.

Collinson J.W., Hammer W.R. *et al*. 2006. Permian-Triassic boundary in the central Transantarctic Mountains, Antarctica. *GSA Bulletin*, **118**, 747–763.

Cornamusini, G., Talarico, F.M. *et al*. 2017. Upper Paleozoic glacigenic deposits of Gondwana: Stratigraphy and paleoenvironmental significance of a tillite succession in Northern Victoria Land (Antarctica). *Sedimentary Geology*, **358**, 51–69.

Crowder, D.F. 1968. Geology of a part of North Victoria Land, Antarctica. *United States Geological Survey Professional Paper*, **600D**, 95–107.

Decombeix, A.-L., Bomfleur, B. *et al*. 2014. New insights into the anatomy, development, and affinities of corystosperm trees from the Triassic of Antarctica. *Review of Palaeobotany and Palynology*, **203**, 22–34.

De Jersey, N.J. 1960. Jurassic spores and pollen grains from the Rosewood coalfield. *Geological Survey of Queensland Publications*, **294**, 1–14.

De Jersey, N.J. 1963. Jurassic spores and pollen grains from the Marburg Sandstone. *Geological Survey of Queensland Publications*, **313**, 1–15.

De Jersey, N.J. and Raine, J.I. 1990. Triassic and earliest Jurassic miospores from the Murihiku Supergroup, New Zealand. *New Zealand Geological Survey Paleontological Bulletin*, **62**, 1–164.

Dickinson, W.R., Geard, L.S. *et al.* 1983. Provenance of North American Phanerozoic sandstones in relation to tectonic setting. *Geological Society of America Bulletin*, **94**, 222–235.

Dow, J.A.S. and Neall, V.E. 1972. Summary of the geology of lower Rennick Glacier, northern Victoria Land. *In*: Adie, R.J. (ed.) *Antarctic Geology and Geophysics*. Universitetsforlaget, Oslo, 339–344.

Dow, J.A.S. and Neall, V.E. 1974. Geology of the Lower Rennick Glacier, northern Victoria Land, Antarctica. *New Zealand Journal of Geology and Geophysics*, **17**, 659–714.

Elliot, D.H. 1975. Gondwana basins in Antarctica. *In*: Campbell, K.S.W. (ed.) *Gondwana Geology*. Australian National University Press, Canberra, 493–536.

ACCEPTED MANUSCRIPT

Downloaded from http://jgs.lyellcollection.org/ at Universitats- und Landesbibliothek Munster on September 16, 2020

Elliot, D.H., Colbert E.H. *et al*. 1970. Triassic tetrapods from Antarctica: evidence for continental drift. *Science*, **169**, 1197–1201.

Elliot, D.H. and Grimes, C.G. 2011. Triassic and Jurassic strata at Coombs Hills, south Victoria Land: stratigraphy, petrology and cross-cutting breccia pipes. *Antarctic Science*, **23**(3), 268-280.

Elliot, D.H., Fanning, C.M. *et al*. 2017. The Permo-Triassic Gondwana sequence, central Transantarctic Mountains, Antarctica: Zircon geochronology, provenance, and basin evolution. *Geosphere*, **13**, 155–178.

Elsner, M., Schöner, R. *et al*. 2013. Reconstruction of the early Mesozoic plate margin of Gondwana by U–Pb ages of detrital zircons from northern Victoria Land, Antarctica. *In*: Harley, S.L., Fitzsimons, I.C.W. and Zhao, Y. (eds) *Antarctica and Supercontinent Evolution*. Geological Society of London Special Publication, **383**, 212–232.

Escapa I.H., Taylor, E.L. *et al.* 2011. Triassic floras of Antarctica: plant diversity and distribution in high paleolatitude communities. *Palaios*, **26**, 522–544.

Farabee, M.J., Taylor, T.N. and Taylor, E.L. 1989. Pollen and spore assemblages from the Falla Formation (Upper Triassic), Central Transantarctic Mountains, Antarctica. *Review of Palaeobotany and Palynology*, **61**, 101-138.

Farabee, M. J., Taylor, E. L. and Taylor, T. N. 1990. Correlation of Permian and Triassic palynomorph assemblages from the central Transantarctic Mountains, Antarctica. *Review of Palaeobotany and Palynology*, **65**, 257-265.

Farabee, M.J., Taylor, E.L. and Taylor, T.N. 1991. Late Permian palynomorphs from the Buckley Formation, central Transantarctic Mountains, Antarctica. *Review of Palaeobotany and Palynology*, **69**, 353–368.

Ferrar, H.T. 1907. Report on the field geology of the region explored during the 'Discovery' expedition 1901-04, National Antarctic Expedition, Natural History 1, Geology, 1-100.

Fielding, C.R., Frank, T.D. *et al.* 2019. Age and pattern of the southern high-latitude continental end-Permian extinction constrained by multiproxy analysis. *Nature Communications*, **10**, 385, https://doi.org/10.1038/s41467-018-07934-z

Filatoff, J. 1975. Jurassic palynology of the Perth Basin, Western Australia. *Palaeontographica Abteilung B*, **154**, 1–113.

Fitzgerald, P.G. and Barrett, P.J. 1986. *Skolithos* in a Permian braided river deposit, southern Victoria Land, Antarctica. *Palaeogeography, Palaeoclimatology, Palaeoecology*, **52**, 237–247.

Forsyth, S.M. 1987. Review of the Upper Parmeener Supergroup. Unpublished Report 1987/01. Tasmania Department of Mines, Hobart.

Fröbisch, J., Angielczyk, K.D. and Sidor, C.A. 2010. The Triassic dicynodont *Kombuisia* (Synapsida, Anomodontia) from Antarctica, a refuge from the terrestrial Permian-Triassic mass extinction. *Naturwissenschaften*, **97**, 187-196.

Gair, H.S., Sturm, A. *et al*. 1969. The geology of northern Victoria Land. *In*: Bushnell, V.C. and Craddock C. (eds) *Geologic Map of Antarctica*. American Geographical Society, New York, folio 12.

ACCEPTED MANUSCRIPT

Downloaded from http://jgs.lyellcollection.org/ at Universitats- und Landesbibliothek Munster on September 16, 2020

Goodge, J.W. 2020. Geological and tectonic evolution of the Transantarctic Mountains, from ancient craton to recent enigma. *Gondwana Research*, **80**, 50-122.

Hammer, W.R. 1986. Takrouna Formation fossils from North Victoria Land. *In*: Stump, E. (ed.) Geological Investigations in Northern Victoria Land. *American Geophysical Union, Antarctic Research Series*, **46**, 243–247.

Hammer, W.R. and Zawiskie, J.M. 1982. Beacon fossils from northern Victoria Land. *Antarctic Journal of the United States*, **17**, 13–14.

Hammer, W.R. 1990. Triassic Terrestrial Vertebrate Faunas of Antarctica. *In*: Taylor, T.N. and Taylor, E.L. (eds) *Antarctic Paleobotany: Its Role in the Reconstruction of Gondwana*. Springer, 42-50.

Harrington, H.J., Wood, B.L. *et al*. 1964. The geology of Cape Hallett-Tucker Glacier district. *In*: Adie, R.J. (ed.) *Antarctic Geology*. North Holland, Amsterdam, 220–228.

Harrington, H.J., Wood, B.L. *et al*. 1967. Topography and geology of the Cape Hallett District, Victoria Land, Antarctica. *New Zealand Geological Survey Bulletin*, **80**, 100 p.

Helby, R.J. and McElroy, C.T. 1969. Microfloras from the Devonian and Triassic of the Beacon group, Antarctica. *New Zealand Journal of Geology and Geophysics*, **12**, 376-382.

Helby, R.J., Morgan, R. and Partridge, A.D. 1987. A palynological zonation of the Australian Mesozoic. *In*: Jell, P.A. (ed.) *Studies in Australian Mesozoic Palynology*. Memoirs of the Association of Australasian Palaeontologists, **4**, 1–94.

Ingersoll, R.V., Bullard, T.F. *et al.* 1984. The effect of grain size on detrital modes: a test of the Gazzi-Dickinson point-counting method. *Journal of Sedimentary Petrology*, **54**, 103–116.

Isbell, J.L. and Askin R.A. 1999. Search for evidence of impact at the Permian-Triassic boundary in Antarctica and Australia: Comment and Reply. *Geology*, **27**, 859-860.

Jell, P.A. 2013. *Geology of Queensland*. Geological Survey of Queensland, 970 p.

John, N. 2014. *Sedimentology and composition of the Takrouna Formation, northern Victoria Land, Antarctica—provenance and depositional environment of a Permian Gondwana basin*. PhD thesis, Friedrich-Schiller-Universität, Jena.

Kemp, E.M., Balme, B.E. *et al.* 1977. Carboniferous and Permian palynostratigraphy in Australia and Antarctica: a review. *BMR Journal of Australian Geology & Geophysics*, **2**, 177–208.

Kerp, H. and Bomfleur, B. 2011. Photography of plant fossils—New techniques, old tricks. *Review of Palaeobotany and Palynology*, **166**, 117–151.

Klimov, L.V. and Soloviev, D.S. 1958. Some characteristics of the geological structure of the coast of Wilkes Land, King George V Coast, and Oates Coast (Eastern Antarctica). *Dokladi Akademii Nauk S.S.S.R.*, **123**, 141–144. (In Russian)

Korsch, R.J. 1974. Petrographic comparison of the Taylor and Victoria Groups (Devonian to Triassic) in south Victoria Land, Antarctica. *New Zealand Journal of Geology and Geophysics*, **17**, 523–541.

Kyle, R.A. 1977. Palynostratigraphy of the Victoria Group of South Victoria Land, Antarctica. *New Zealand Journal of Geology and Geophysics*, **20**, 1081–1102.

ACCEPTED MANUSCRIPT

Downloaded from http://jgs.lyellcollection.org/ at Universitats- und Landesbibliothek Munster on September 16, 2020

Kyle, R.A. and Fasola, A. 1978. Triassic palynology of the Beardmore Glacier area of Antarctica. *Palinología, Número Extraordinario*, **1**, 313–319.

Kyle, R.A. and Schopf, J.M. 1982. Permian and Triassic palynostratigraphy of the Victoria Group, Transantarctic Mountains. *In*: Craddock, C. (ed.), *Antarctic Geoscience*. The University of Wisconsin Press, Madison, 649–659.

Laird, M.G. and Bradshaw, J.D. 1981. Permian tillites of North Victoria Land. *In*: Hambrey, M.J. and Harland, W.B. (eds), *Earth's pre-Pleistocene Glacial Record*. Cambridge University Press, 237–240.

Le Couteur, P.C. and Leitch, E.C. 1964. Preliminary report on the geology of an area south-west of Upper Tucker Glacier, northern Victoria Land. *In*: Adie, R.J. (ed.) *Antarctic Geology*. North Holland, Amsterdam, 229–236.

Looy C.V., Twitchett, R.J. *et al*. 2001. Life in the end-Permian dead zone. *PNAS*, **98**, 7879-7883.

Masood, K.R., Taylor, T.N. *et al*. 1994. Palynology of the Mackellar Formation (Beacon Supergroup) of East Antarctica. *Review of Palaeobotany and Palynology*, **83**, 329–337.

Mays, C., Vajda, V. *et al.* 2020. Refined Permian–Triassic floristic timeline reveals early collapse and delayed recovery of south polar terrestrial ecosystems. *GSA Bulletin*, **132**, 1489-1513.

McBride, E.F. 1963. A classification of common sandstones. *Journal of Sedimentary Research*, **33**, 664-669.

McElroy, C.T. 1969. Comparative lithostratigraphy of Gondwana sequences, eastern Antarctica and Antarctica. *In*: Amos, A.H. (ed.) *Gondwana Stratigraphy*. UNESCO, Paris, 441–466.

McKelvey, B.C. and Walker, B.C. 1983. Late Palaeozoic glacigene strata in northern Victoria Land. *In*: Oliver, R.L., James, P.R. and Jago, J.B. (eds) *Antarctic Earth Science*. Cambridge University Press, 226.

McLeod, I.R. 1964. Geological observations in Oates Land. *In*: Adie, R.J. (ed.) *Antarctic Geology*. North Holland, Amsterdam, 482–486.

McManus, H.A., Taylor, E.L. *et al*. 2002. A petrified *Glossopteris* flora from Collinson Ridge, central Transantarctic Mountains: Late Permian or Early Triassic? *Review of Palaeobotany and Palynology*, **120**, 233–246.

Miller, M.F. and Collinson, J.W. 1994. Trace fossils from Permian and Triassic braided stream deposits, central Transantarctic Mountains. *Palaios*, **9**, 605–610.

Mörs, T., Niedzwiedzki, G. *et al*. 2019. First evidence of a tetrapod footprint from the Triassic of northern Victoria Land, Antarctica. *Polar Research*, **38**, 3438, http://dx.doi.org/10.33265/polar.v38.3438

Musumeci, G., Pertusati, P.C., Ribecai, C. and Meccheri, M. 2006. Early Jurassic fossiliferous black shales in the Exposure Hill Formation, Ferrar Group of northern Victoria Land, Antarctica. *Terra Antartica Reports*, **12**, 91–98.

Oh, C., Park, T.-Y.S. *et al*. 2016. Triassic *Kykloxylon* wood (Umkomasiaceae, Gymnospermopsida) from Skinner Ridge, northern Victoria Land, East Antarctica. *Review of Palaeobotany and Palynology*, **233**, 104–114.

ACCEPTED MANUSCRIPT

Downloaded from http://jgs.lyellcollection.org/ at Universitats- und Landesbibliothek Munster on September 16, 2020

Peecook, E.R., Smith, R.M.H. and Sidor, C.A. 2019. A novel archosauromorph from Antarctica and an updated review of a high-latitude vertebrate assemblage in the wake of the end-Permian mass extinction. *Journal of Vertebrate Paleontology*, **38**, e1536664. doi: https://doi.org/10.1080/02724634.2018.1536664.

Playford, G.J. 1990. Proterozoic and Paleozoic palynology of Antarctica: a review. *In*: Taylor, T.N. and Taylor, E.L. (eds) *Antarctic Paleobotany: Its Role in the Reconstruction of Gondwana*. Springer, 51–70.

Price, P.L. 1997. Permian to Jurassic palynostratigraphic nomenclature of the Bowen and Surat Basins. *In*: Green, P.M. (ed.) *The Surat and Bowen Basins, South-east Queensland*. Queensland Department of Mines and Energy, Brisbane, 137–178.

Rastall, R.H. and Priestley R.E. 1921. The slate-graywacke formation of Robertson Bay. *British Antarctic (Terra Nova) Expedition 1910, Natural History Reports, Geology*, **1**, 121–129.

Retallack, G.J. and Krull, E.S. 1999. Landscape ecological shift at the Permian-Triassic boundary in Antarctica. *Australian Journal of Earth Sciences*, **46**, 785-812.

Ribecai C. 2007. Early Jurassic miospores from Ferrar Group of Carapace Nunatak, South Victoria Land, Antarctica. *Review of Palaeobotany and Palynology*, **144**, 3-12.

Ricker, J. 1964. Outline of the Geology between Mawson and Priestley Glaciers, Victoria Land. *In* Adie, R.J., *ed. Antarctic Geology*. *SCAR Proceedings 1963*. Amsterdam: North Holland Publishing, 265–275.

Schöner, R. and John, N. 2014. Sedimentological field investigations on the Takrouna Formation (Permian, Beacon Supergroup) in northern Victoria Land, Antarctica. *Polarforschung*, **84**, 49–58.

Schöner, R., Bomfleur, B. *et al*. 2011. A systematic description of the Triassic to Lower Jurassic Section Peak Formation in North Victoria Land (Antarctica). *Polarforschung*, **80**, 71–87.

Sidor, C.A., Ross, D. and Hammer, W.R. 2008. A new Triassic temnospondyl from Antarctica and a review of Fremouw Formation biostratigraphy. *Journal of Vertebrate Paleontology*, **28**, 656–663.

Skinner, D.N.B. 1981. Possible Permian glaciation in north Victoria Land, Antarctica. *Geologisches Jahrbuch*, **B41**, 261–266.

Soloviev, D.S. 1960. The lower Palaeozoic metamorphic slates of the Oates Coast. Naucho-issledovatelsky Institut Geologii Antarktiki, **113**. [in Russian]

Sturm, A. and Carryer, S.J. 1970. Geology of the region between Matusevich and Tucker glaciers, northern Victoria Land. *New Zealand Journal of Geology and Geophysics*, **13**, 408–435.

Tasch, P. and Lammons, J.M. 1978. Palynology of some lacustrine interbeds of the Antarctic Jurassic. *Palinologia*, Núm. Extraordinario **1**, 455–460.

Tessensohn, F. and Mädler, K. 1987. Triassic plant fossils from North Victoria Land, Antarctica. *Geologisches Jahrbuch*, **B66**, 187–201.

Unverfärth, J., Mörs, T., and Bomfleur, B. *in press*. Palynological evidence supporting widespread synchronicity of Early Jurassic silicic volcanism throughout the Transantarctic Basin. *Antarctic Science*, doi:10.1017/S0954102020000346

ACCEPTED MANUSCRIPT

Downloaded from http://jgs.lyellcollection.org/ at Universitats- und Landesbibliothek Munster on September 16, 2020

Walker, B.C. 1983. The Beacon Supergroup of northern Victoria Land, Antarctica. *In*: Oliver, R.L., James, P.R. and Jago, J.B. (eds) *Antarctic Earth Science*. Cambridge University Press, 211–214.

Zawiskie, J.M., Collinson, J.W. and Hammer, W.R. 1983. Trace fossils of the Permian-Triassic Takrouna Formation, northern Victoria Land, Antarctica. *In*: Oliver, R.L., James, P.R. and Jago, J.B. (eds) *Antarctic Earth Science*. Cambridge University Press, 215–220.

Zhang, W. and Grant-Mackie, J.A. 2001. Late Triassic-Early Jurassic palynofloral assemblages from Murihiku strata of New Zealand, and comparisons with China. *Journal of the Royal Society of New Zealand*, **31**, 575–683.

ACCEPTED MANUSCRIPT

Downloaded from http://jgs.lyellcollection.org/ at Universitats- und Landesbibliothek Munster on September 16, 2020

## Figure captions

**Fig. 1** [*mid-width figure*]**.** Geographic setting of the study area (left) and visited sections in the Helliwell Hills (right), northern Victoria Land, East Antarctica. Locality numbers (locality codes in parentheses): **1–6** all around Helliwell Camp (see also Fig. S2): northwest slope (HCNW: **1**), northeast slope (HCNE: **2**), campsite cliff (HCCL: **3**), peak plateau (HCtop: **4**), southeast slope (HCSE: **5**), south (HCS: **6**); **7**: unnamed ridge about halfway between Mount Remington and Mount Bresnahan (BS); **8**: unnamed ridge ~3 km north of Mount Van der Hoeven (MVH); **9**: unnamed slope ~2 km north of Mount Van der Hoeven; **10–13** all in Boggs Valley: top (BVT: **10**), main site (BV: **11**), unnamed mesa west of Boggs Valley head (BVM: **12**), and north-south-trending ridge at the western head end of Boggs Valley (BVR: **13**).

**Fig. 2** [*full-page figure, ideally verso*]. Field images and fossil content of the Early Triassic Van der Hoeven Formation in the Helliwell Hills, northern Victoria Land. (**a**) view NNW across the top part of the BS section at an unnamed nunatak about halfway between Mount Remington and Mount Bresnahan (thickness of visible part of section below sill ~60 m); (**b**) variably coloured silt- and fine-grained sandstone in the basal part of the Van der Hoeven Formation (BS09) at the BS section; (**c**) view NW across the provisional type section (section MVH) of the Van der Hoeven Formation at an unnamed knob ~1.5 km north of Mount Van der Hoeven (thickness of visible part of section below sill ~50 m); (**d**) palaeosol in the middle part of the type section, with root horizon and nodular concretion (arrow); (**e**) laterally extensive body of tabular, dune-sized cross-beds of pebbly sandstone overlying the intraclastic conglomerate at the type section; (**f**) stacks of trough- and tabular-cross-bedded sandstone bodies exposed in the lowermost cliff at the Helliwell Hills campsite section (HCCL); (**g**) vertical *Skolithos* burrows, HCCL section; (**h**) *Cylindricum*-type sand plugs in an intensely bioturbated mudstone intraclast at the type section; (**i**) *Diplichnites* trackway, HCCL section; (**j**) meniscate-backfilled *Scoyenia* burrow, HCCL section. Scale bars: (g) = 10 cm, (h, i) = 2 cm, (j) = 1 cm; note hammes for scale in (e) and (f) are highlighted with black contours.

**Fig. 3** [*mid-width figure*]. View west onto the type section of the Helliwell Formation and nearby exposures surrounding an unnamed mesa 3 km east of Dziura Nunatak in the

ACCEPTED MANUSCRIPT

Downloaded from http://jgs.lyellcollection.org/ at Universitats- und Landesbibliothek Munster on September 16, 2020

northern Helliwell Hills, showing stratigraphic units, measured sections, and important macro- and microfossil sites; see Fig. 7 for legend of symbols in lower panel; thickness of exposed section from base to top (below sill) is ~300 m.

**Fig. 4** [*full-page figure, ideally verso*]. Field images and fossil content of the Middle to Late Triassic Helliwell Formation in the northern Helliwell Hills, northern Victoria Land. (**a**) bed of fine-grained sandstone (HCSE01o) with symmetrical ripples (on float specimen), exposed among slope debris near the base of the Helliwell Formation at the type section; (**b**) cliff-forming intercalation of fine-grained volcaniclastic sandstone (HCSE04–05) in the lower part of the Helliwell Formation at the type section, with person for scale (arrow); (**c**) detail of the cliff exposure shown in (b), showing erosive channel fill (HCSE04) with abundant coal and carbonaceous mudstone intraclasts; (**d**) view SW up the upper half of the HCNE section onto the mesa-forming remnant of a Ferrar sill, with a *c.* 1-m-thick exposure of fine-grained sandstone and carbonaceous mudstone in the foreground; (**e**) conifer leaf *Heidiphyllum elongatum* from a carbonaceous mudstone bed (HCSE10) near the top of the Helliwell Formation at the type section; (**f**) a small lycopsid sporophyll (*Lepacyclotes* sp.) from the central part (HCSE08) of the Helliwell Formation at the type section; (**g**) large slab of a silicified *Kykloxylon* trunk collected from surface debris in the central part of the Helliwell Formation about half-way upslope the HCNE sector at the type section; (**h**) top of the Helliwell Formation at the type section, truncated by the disconformably overlying Section Peak Formation (HCSE12) with conglomeratic basal layer and abundant fossil wood (arrows) in turn capped by a cliff-forming sill intrusion. Scale bars: (e) = 1 cm, (f) = 2 mm, (g) = 5 cm; hammers for scale in (c) and (d) highlighted with white contours.

**Fig. 5** [*mid-width figure*]**.** Petrography of selected sandstone samples from different stratigraphic units of the Beacon Supergroup in the Helliwell Hills, lower Rennick Glacier. (**a**) Diagrams below show ternary classifications of the studied sandstone samples following McBride (1963) (*left*) and Dickinson *et al.* (1983) (*right*). (**b**) coarse-grained, submature subarkose (sample NVL1116) from the upper part of the Van der Hoeven Formation at the HCCL section (equivalent to bed HCCL09); (**c**) fine-grained, moderately sorted, immature feldspathic litharenite (sample NVL116) from the lower part of the Helliwell Formation at the type section (equivalent to bed HCSE07). Colour coding according to Fig. 1. Scale bars: (b) = 500 µm, (c) = 200 µm.

ACCEPTED MANUSCRIPT

Downloaded from http://jgs.lyellcollection.org/ at Universitats- und Landesbibliothek Munster on September 16, 2020

**Fig. 6** [*full-page figure, ideally verso*]. Selected palynomorphs from the Takrouna Formation (a–h), Van der Hoeven Formation (i–r), Helliwell Formation (s–ac) and Section Peak Formation (ad–af) in the Helliwell Hills, lower Rennick Glacier, East Antarctica, with slide number and England Finder coordinates. (**a**) *Protohaploxypinus limpidus*, GXI-BS04-10, O29/3; (**b**) *Protohaploxypinus amplus*, GXI-BS04-11, J34/2; (**c**) *Striatopodocarpites* sp., GXI-BS04-10- P27; (**d**) *Protohaploxypinus* sp., GXI-BS04-11, M3; (**e**) *Praecolpatites sinuosus*, GXI-BS04-10, W51; (**f**) *Marsupipollenites triradiatus*, GXI-BS04-13, F69/3; (**g**) *Dulhuntyispora dulhuntyi*, GXI-BS04-1, P28/1; (**h**) *Dulhuntyispora parvithola*, GXI-BS04-7, D46; (**i**) *Densoisporites* sp. cf. *D. nejburgii*, GXI-BS09-LF2, P40/4; (**j**) *Lundbladispora willmottii*, GXI-BS09-1, E62; (**k**) *Limatulasporites* sp. cf. *L. limatulus*, GXI-BS09-1, S69/4; (**l**) *Retusotriletes nigritellus*, GXI-MVH-16, X63/4; (**m**) *Endosporites papillatus*, GXI-BS09-1, G56/4; (**n**) *Playfordiaspora crenulata*, GXI-MVH-13, K38/1; (**o**) *Scheuringipollenites ovatus*, GXI-MVH-12, R44; (**p**) *Hamiapollenites insculptus*, GXI-MVH-17, D43/2; (**q**) *Reduviasporonites catenulatus*, GXI-BS09-MVH-17, G43/2; (**r**) *Aratrisporites tenuispinosus*, GXI-HCSE01o-1, T42/3; (**s**) *Aratrisporites fischeri*, GXI-HCSE01o-1, H51/4; (**t**) *Lundbladispora brevicula*, GXI-HCSE01o-4, Q15; (**u**) *Equisetosporites steevesii*, GXI-HCSE01o-1, L48/1; (**v**) *Staurosaccites quadrifidus*, GXI-HCSE01o-LF4, S30/2; (**w**) *Alisporites australis*, GXI-HCSE10-7, Q68/1; (**x**) *Platysaccus queenslandii*, GXI-HCSE10-7, T39/2; (**y**) *Limbosporites denmeadii*, GXI-HCSE08-5, C28/1; (**z**) *Craterisporites rotundus*, GXI-HCSE10-14, O63; (**aa**) *Stereisporites antiquasporites*, GXI-HCSE10-14, Y55/3; (**ab**) *Annulispora folliculosa*, GXI-HCSE08-6, E41/4; (**ac**) *Annulispora microannulata*, GXI-HCSE10c-1, X41; (**ad**) *Araucariacites* sp. cf. *A. australis*, GXI-HCtop-2, D56/3; (**ae**); *Podocarpidites* sp. cf. *P. major*, GXI-HCtop-3, Y63/1; (**af**) *Matonisporites* sp. cf. *M. phlebopteroides*, GXI-HCtop-2, W67; scale bars = 25 µm.

**Fig. 7** [*single-column figure*]. Sedimentary log of the BS section exposed at an unnamed nunatak half-way between Mount Remington and Mount Bresnahan in the central Helliwell Hills, northern Victoria Land; colours indicate dominant general colouration and relative colour changes; c = clay, s = silt, Sf = fine-grained sandstone, Sm = medium-grained sandstone, Sc = coarse-grained sandstone, C = conglomerate.

**Fig. 8** [*single-column figure*]. Composite sedimentary log of the HCCL, HCSE, and HCtop sections exposed along the eastern flank of an unnamed inselberg c. 3 km east of Dziura Nunatak, northern Helliwell Hills, northern Victoria Land; see Fig. 7 for legend; colours

ACCEPTED MANUSCRIPT

Downloaded from http://jgs.lyellcollection.org/ at Universitats- und Landesbibliothek Munster on September 16, 2020

indicate dominant general colouration and relative colour changes; c = clay, s = silt, Sf = fine-grained sandstone, Sm = medium-grained sandstone, Sc = coarse-grained sandstone, C = conglomerate; brown line separating HCSE12 and HCtop01 represents the ~50-m-thick, cliff-forming Ferrar sill.

**Fig. 9** [*full-page-width figure*]. Idealized composite sedimentary log for the Beacon Supergroup and Ferrar Group deposits in the far North of Victoria Land, East Antarctica; additional data on the Lanterman Formation, Takrouna Formation and Kirkpatrick Basalt adopted from Skinner *et al*. (1981), John (2014), and Cornamusini *et al*. (2017); *x* and *y* indicate potential gaps of unknown stratigraphic thickness; note that colours for columns in central part of image (Stratigraphic coverage of outcrop regions) is according to stratigraphic unit (see Fig. 1) and not to dominant lithologies.

**Fig. 10** [*full-page-width figure*]. Comparison of stratigraphic units of the Beacon Supergroup and overlying Jurassic rock units across selected outcrop regions of the Transantarctic basin system and Tasmania; data for Beardmore Glacier area (central Transantarctic Mountains) and Convoy Range/Allan Hills (southern Victoria Land) from Barrett (1991) and Elliot *et al.* (2017); for Eisenhower Range to lower Rennick Glacier area (northern Victoria Land) from Bomfleur *et al.* (2014a, b) and Cornamusini *et al*. (2017) with modifications in bold according to this study; and for Tasmania from Forsyth (1987) and Bromfield *et al*. (2007).

ACCEPTED MANUSCRIPT

Downloaded from http://jgs.lyellcollection.org/ at Universitats- und Landesbibliothek Munster on September 16, 2020

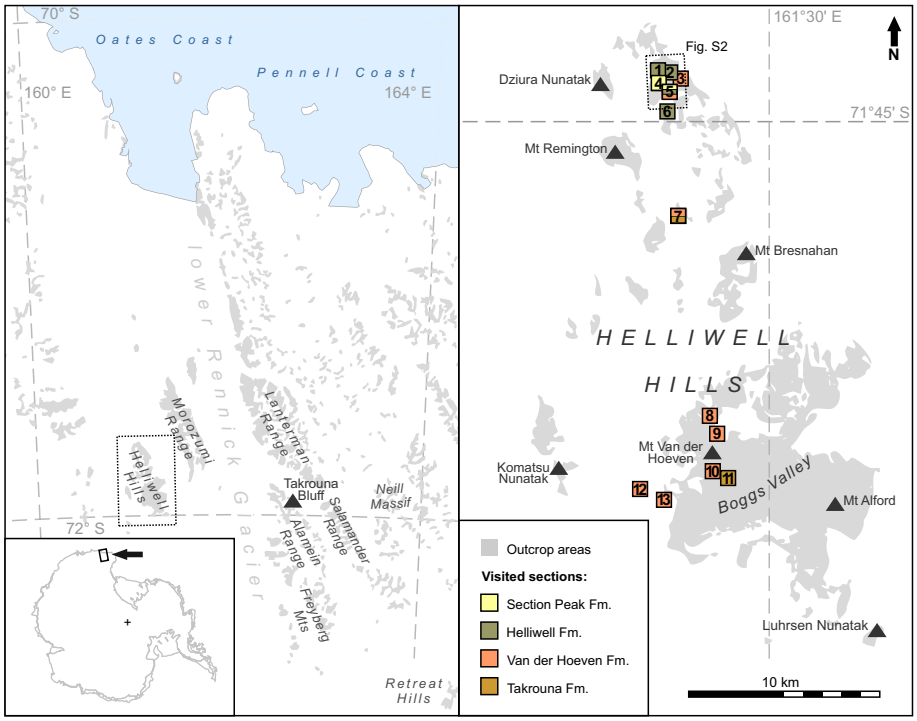


ACCEPTED MANUSCRIPT

Downloaded from http://jgs.lyellcollection.org/ at Universitats- und Landesbibliothek Munster on September 16, 2020

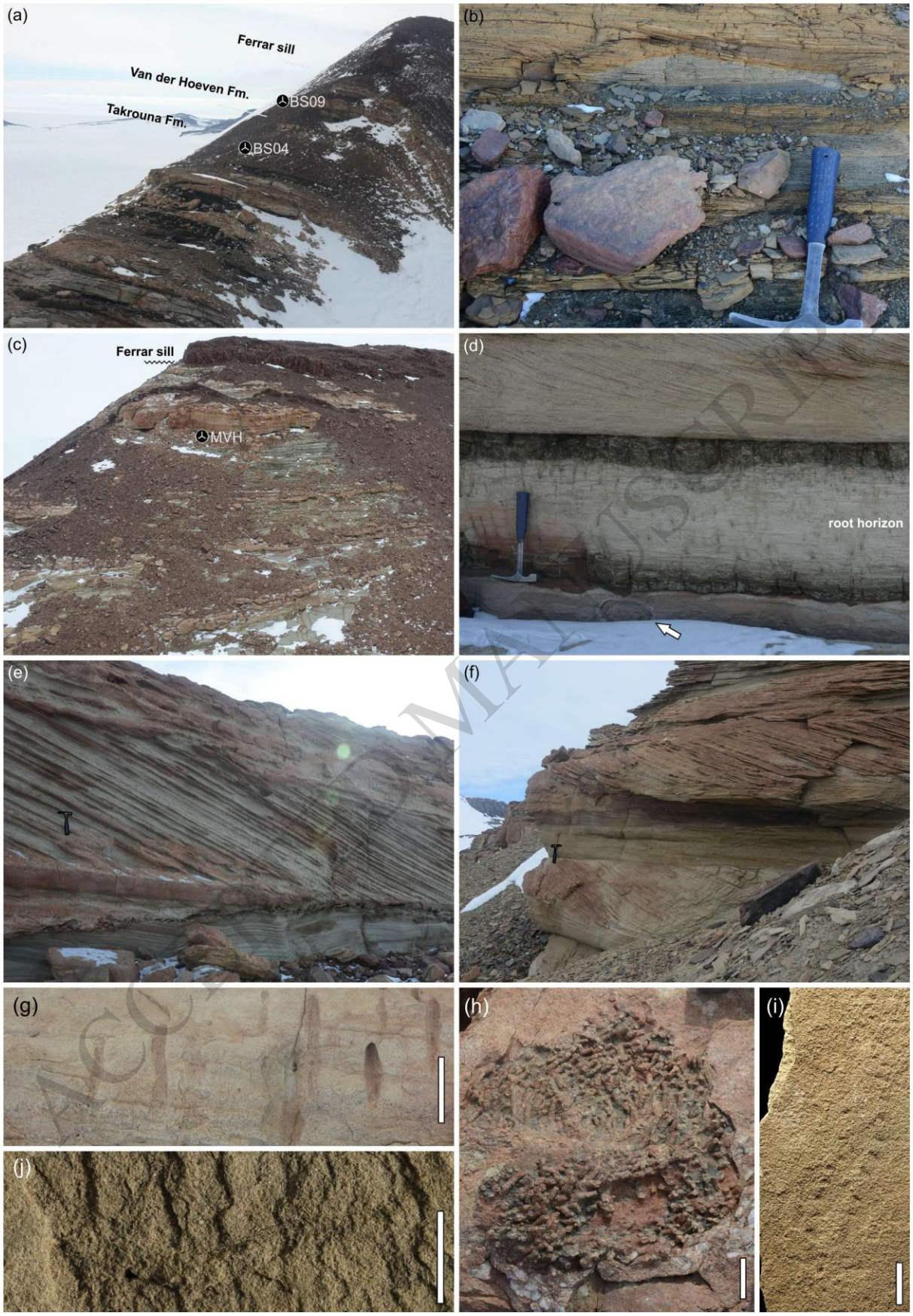


ACCEPTED MANUSCRIPT

Downloaded from http://jgs.lyellcollection.org/ at Universitats- und Landesbibliothek Munster on September 16, 2020

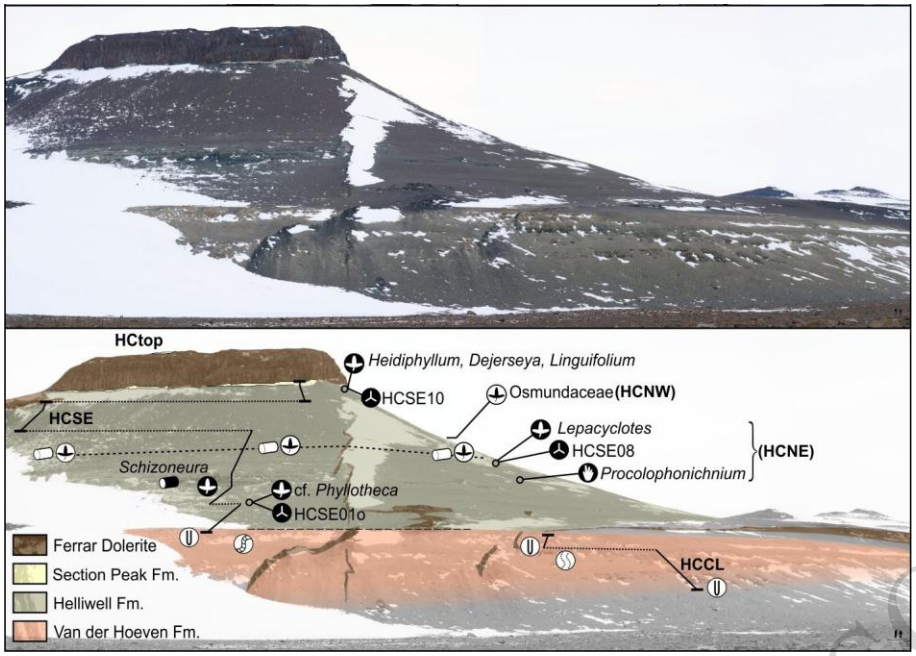


ACCEPTED MANUSCRIPT

Downloaded from http://jgs.lyellcollection.org/ at Universitats- und Landesbibliothek Munster on September 16, 2020

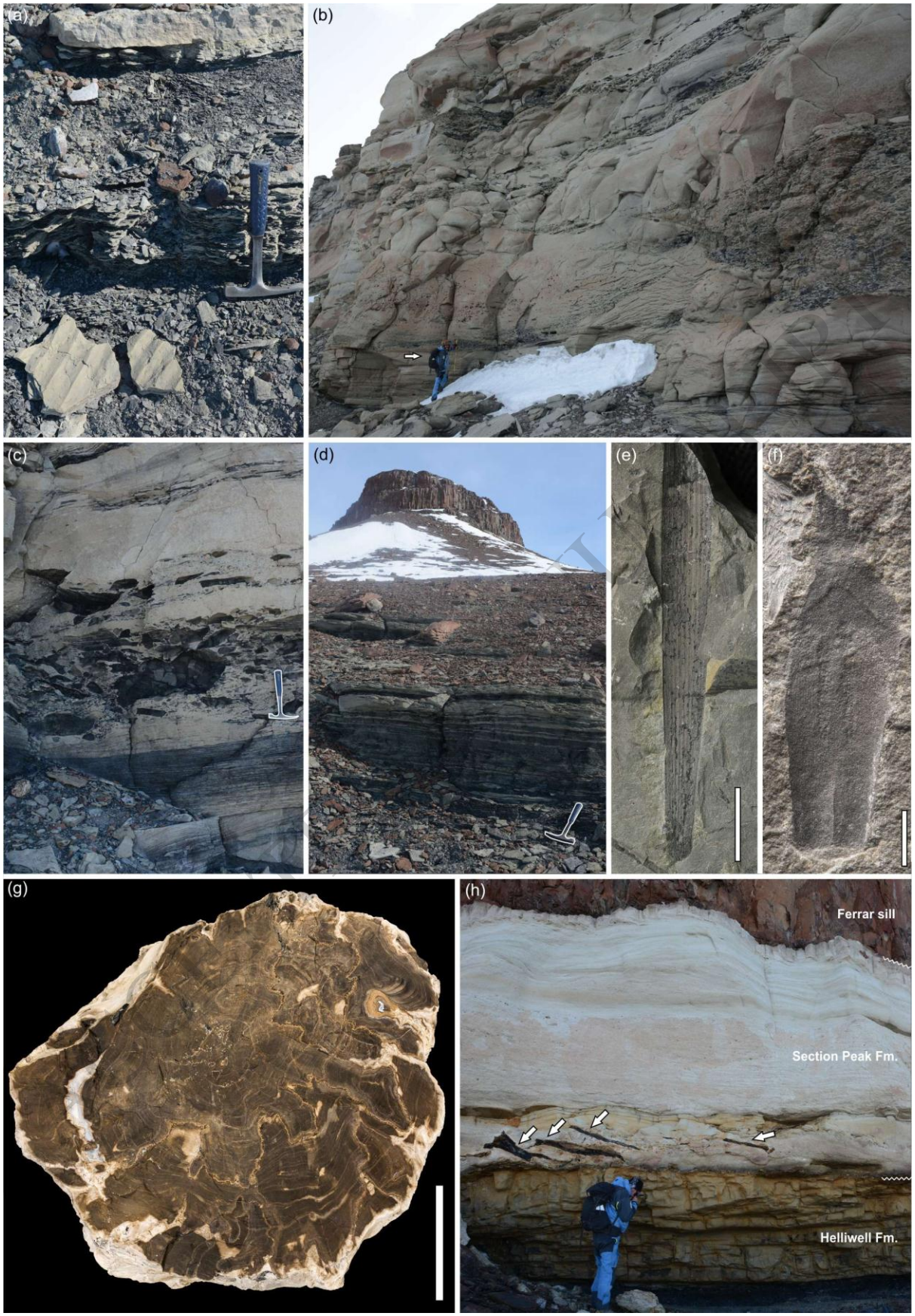

Downloaded from http://jgs.lyellcollection.org/ at Universitats- und Landesbibliothek Munster on September 16, 2020

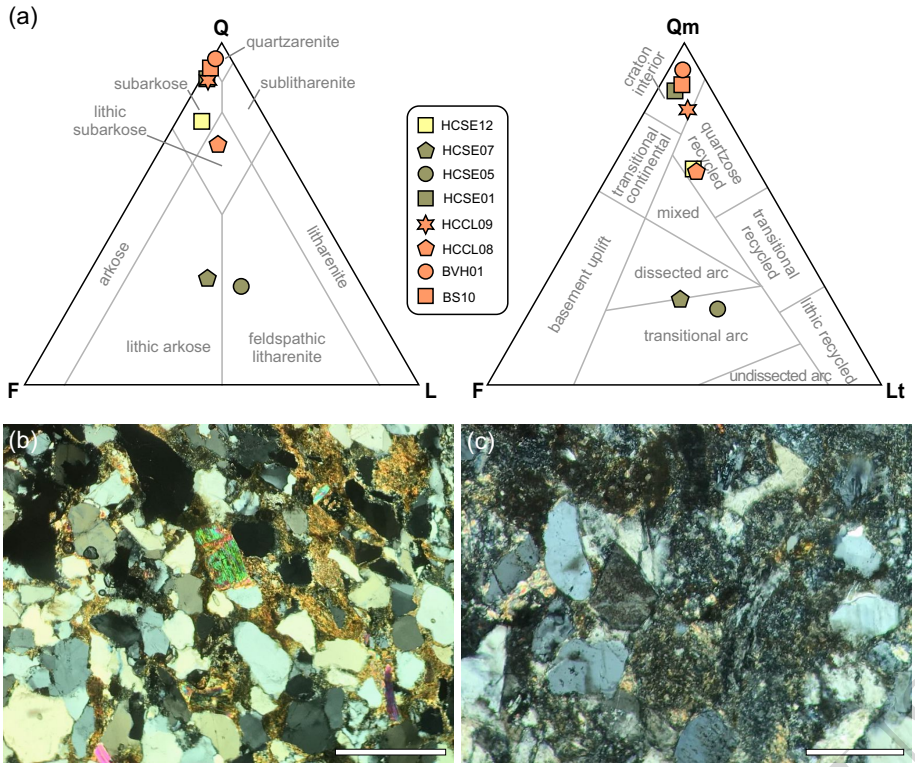


ACCEPTED MANUSCRIPT

Downloaded from http://jgs.lyellcollection.org/ at Universitats- und Landesbibliothek Munster on September 16, 2020

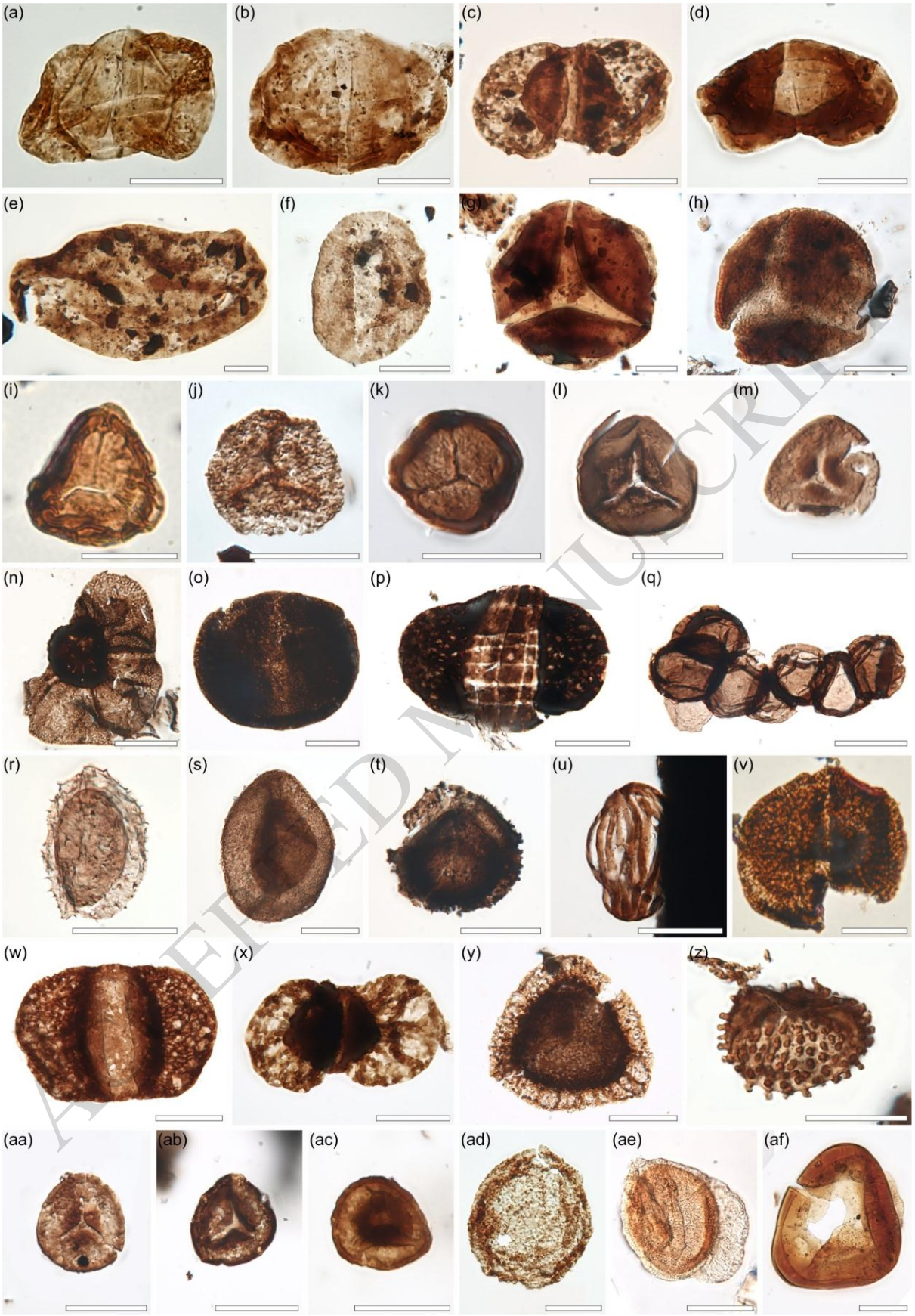


ACCEPTED MANUSCRIPT

Downloaded from http://jgs.lyellcollection.org/ at Universitats- und Landesbibliothek Munster on September 16, 2020

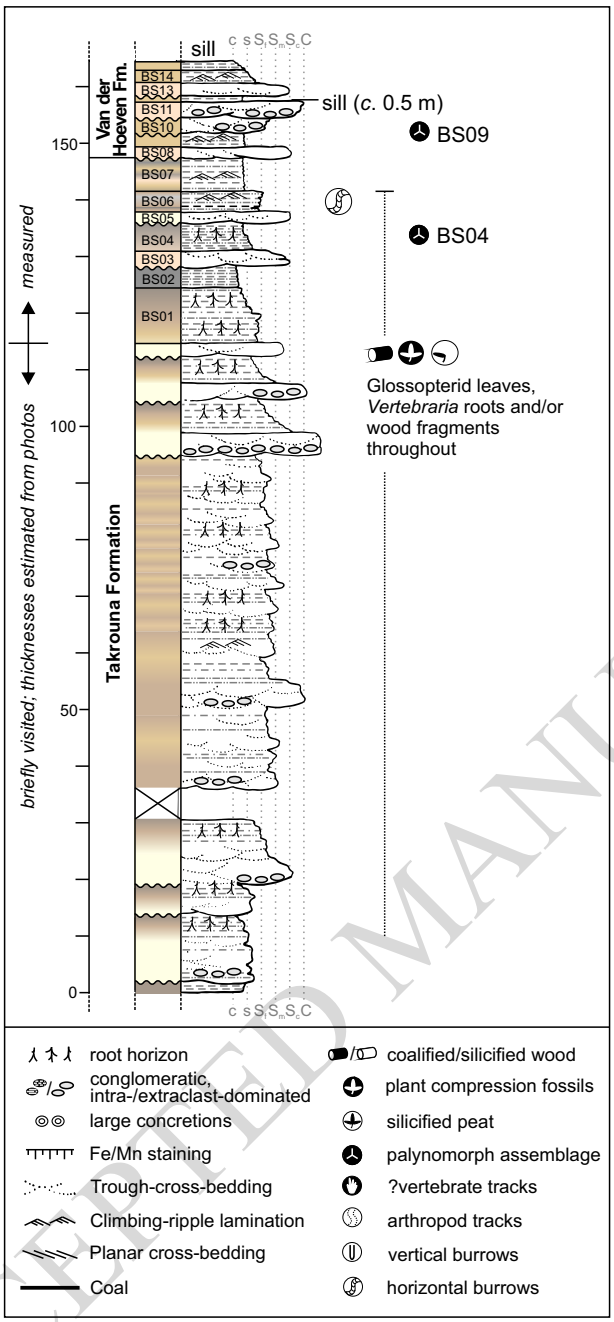


ACCEPTED MANUSCRIPT

Downloaded from http://jgs.lyellcollection.org/ at Universitats- und Landesbibliothek Munster on September 16, 2020

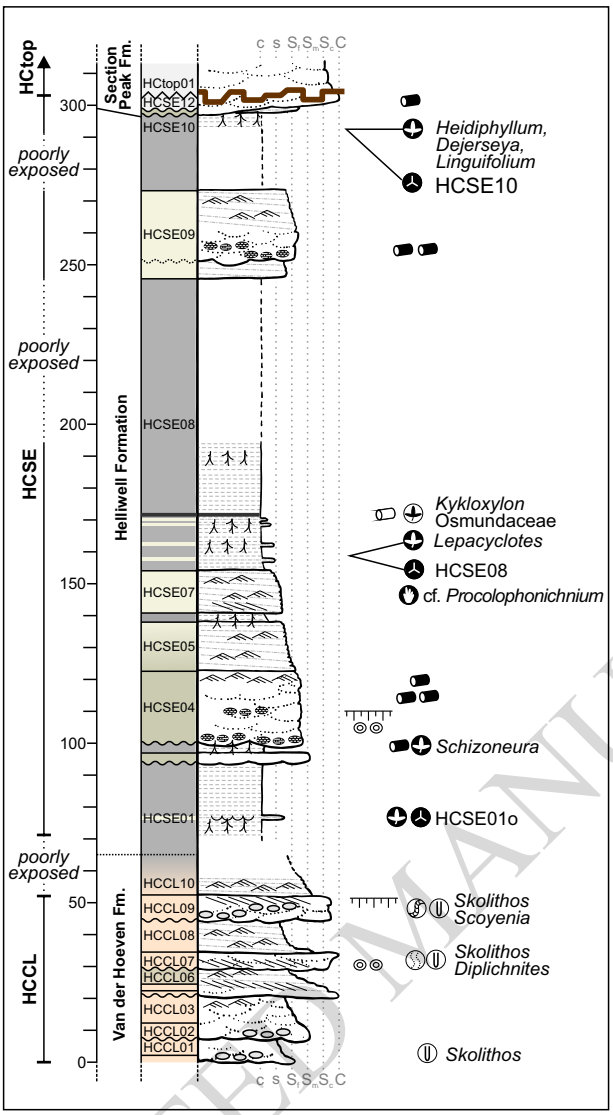


ACCEPTED MANUSCRIPT

Downloaded from http://jgs.lyellcollection.org/ at Universitats- und Landesbibliothek Munster on September 16, 2020

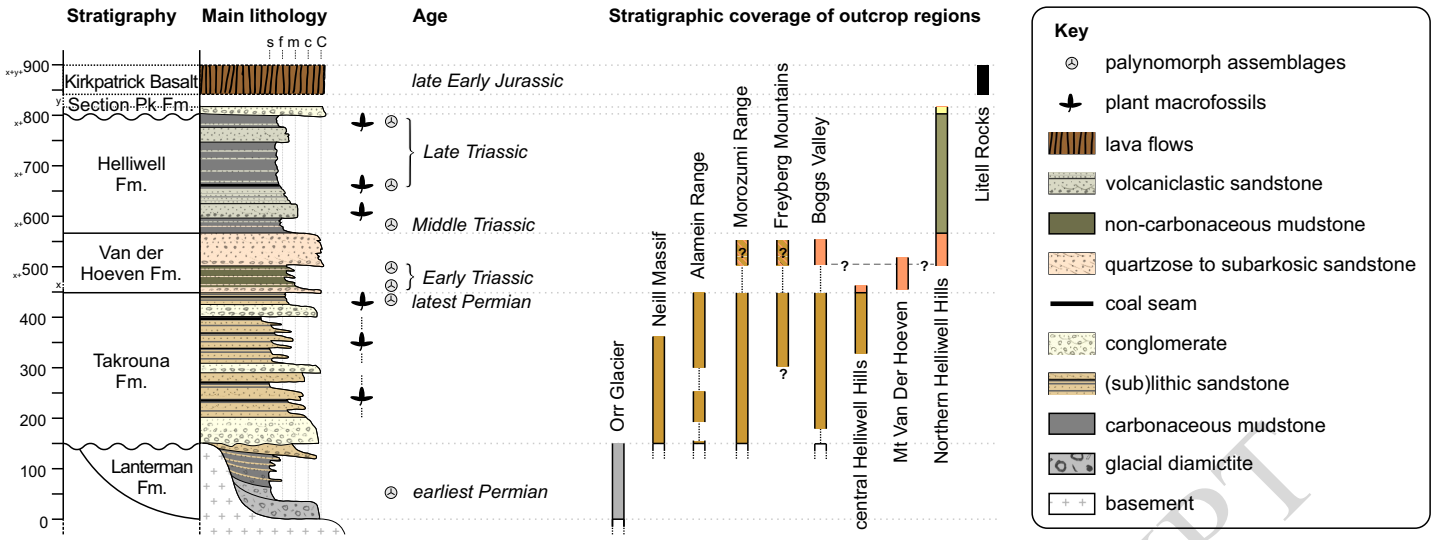


ACCEPTED MANUSCRIPT

Downloaded from http://jgs.lyellcollection.org/ at Universitats- und Landesbibliothek Munster on September 16, 2020

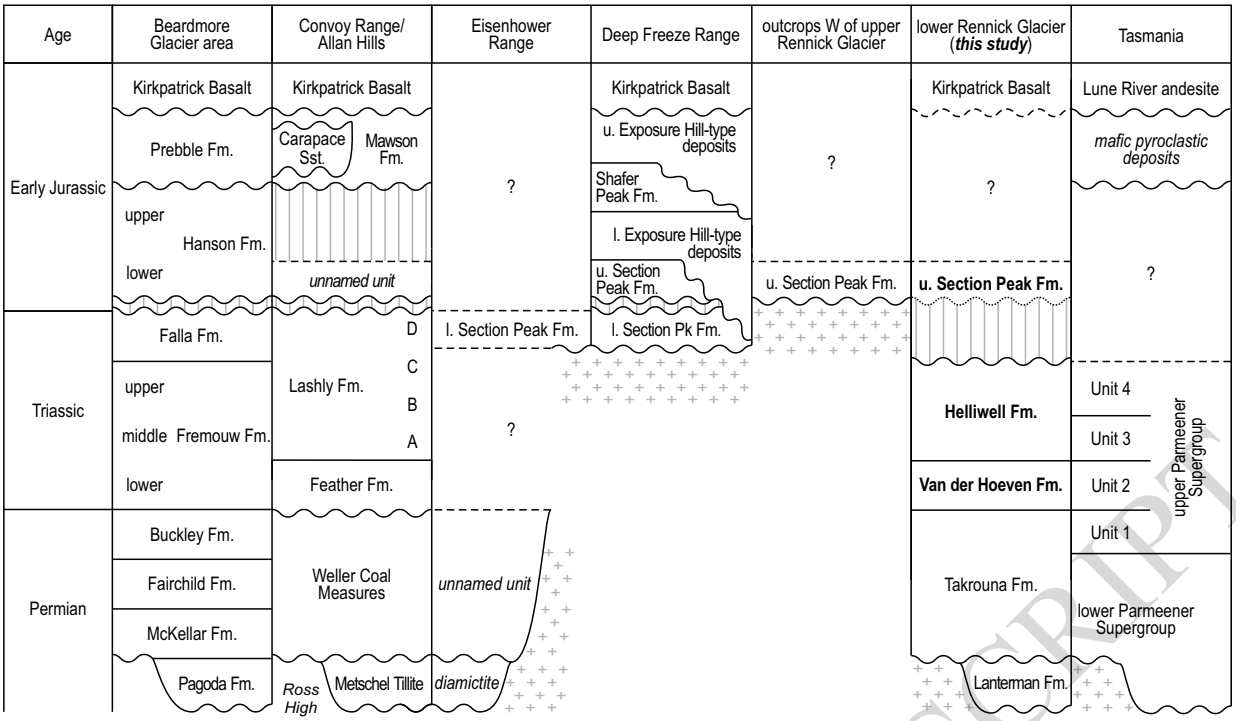


ACCEPTED MANUSCRIPT